

Two-zero Textures of the Majorana Neutrino Mass Matrix and Current Experimental Tests

Harald Fritzsch ^a, Zhi-zhong Xing ^{b *}, Shun Zhou ^{c †}

^aPhysik-Department, Ludwig-Maximilians-Universität, 80333 München, Germany

^bInstitute of High Energy Physics, Chinese Academy of Sciences, Beijing 100049, China

^cMax-Planck-Institut für Physik (Werner-Heisenberg-Institut), 80805 München, Germany

Abstract

In view of the latest T2K and MINOS neutrino oscillation data which hint at a relatively large θ_{13} , we perform a systematic study of the Majorana neutrino mass matrix M_ν with two independent texture zeros. We show that three neutrino masses (m_1, m_2, m_3) and three CP-violating phases (δ, ρ, σ) can fully be determined from two neutrino mass-squared differences ($\delta m^2, \Delta m^2$) and three flavor mixing angles ($\theta_{12}, \theta_{23}, \theta_{13}$). We find that seven patterns of M_ν (i.e., $\mathbf{A}_{1,2}$, $\mathbf{B}_{1,2,3,4}$ and \mathbf{C}) are compatible with current experimental data at the 3σ level, but the parameter space of each pattern is more strictly constrained than before. We demonstrate that the texture zeros of M_ν are stable against the one-loop quantum corrections, and there exists a permutation symmetry between Patterns \mathbf{A}_1 and \mathbf{A}_2 , \mathbf{B}_1 and \mathbf{B}_2 or \mathbf{B}_3 and \mathbf{B}_4 . Phenomenological implications of M_ν on the neutrinoless double-beta decay and leptonic CP violation are discussed, and a realization of those texture zeros by means of the Z_n flavor symmetries is illustrated.

PACS numbers: 14.60.Lm, 14.60.Pq

*E-mail: xingzz@ihep.ac.cn

†E-mail: zhoush@mppmu.mpg.de

1 Introduction

Compelling evidence in favor of neutrino oscillations has been accumulated from a number of solar, atmospheric, reactor and accelerator neutrino experiments since 1998 [1]. We are now convinced that the three known neutrinos have nonzero and nondegenerate masses, and their flavor states can convert from one kind to another. In particular, two neutrino mass-squared differences ($\delta m^2, \Delta m^2$) and two flavor mixing angles (θ_{12}, θ_{23}) have been determined to a reasonably good degree of accuracy from currently available experimental data. In spite of this progress made in neutrino physics, our quantitative knowledge about the properties of massive neutrinos remain quite incomplete — for instance, the absolute mass scale of three neutrinos, the sign of Δm^2 and the smallest flavor mixing angle θ_{13} are still unknown. Although the nature of massive neutrinos is also an open question, we assume them to be the Majorana particles. In this case the 3×3 Majorana neutrino mass matrix M_ν is symmetric, and the corresponding 3×3 flavor mixing matrix V contains three CP-violating phases (δ, ρ, σ) which are entirely unrestricted by current experimental data.

The T2K [2] and MINOS [3] accelerator neutrino experiments have recently announced their preliminary data on the appearance $\nu_\mu \rightarrow \nu_e$ oscillation, which hints at a relatively large value of θ_{13} . If this mixing angle is confirmed to be not very small by new data from these two experiments and from the upcoming reactor antineutrino experiments (e.g., the Double Chooz experiment in France [4], the Daya Bay experiment in China [5] and the RENO experiment in Korea [6]), it will be a great news to the long-baseline neutrino oscillation experiments which aim at a determination of the sign of Δm^2 and the magnitude of the Dirac CP-violating phase δ . The observed values of relevant neutrino flavor parameters may then allow us to reconstruct the Majorana neutrino mass matrix M_ν in the flavor basis where the charged-lepton mass matrix M_l is diagonal: $M_\nu = V \widehat{M}_\nu V^T$, where $\widehat{M}_\nu = \text{Diag}\{m_1, m_2, m_3\}$ with m_i (for $i = 1, 2, 3$) being the neutrino masses, and V is just the 3×3 neutrino mixing matrix.

In the lack of a convincing flavor theory, at least five approaches have so far been tried to study the flavor problems of massive neutrinos [7]: (a) radiative mechanisms, (b) texture zeros, (c) flavor symmetries, (d) seesaw mechanisms, and (e) extra dimensions. Some of them are certainly correlative. For example, the neutrino mass matrix M_ν may have a few texture zeros as a natural consequence of an underlying flavor symmetry in a given model with or without the seesaw mechanism. Such texture zeros are phenomenologically useful in the sense that they guarantee the calculability of M_ν from which both the neutrino mass spectrum and the flavor mixing pattern can more or less be predicted. Note that texture zeros of a fermion mass matrix dynamically mean that the corresponding matrix elements are sufficiently suppressed in comparison with their neighboring counterparts [8], and they can help us to establish some simple and testable relations between flavor mixing angles and fermion mass ratios — if such relations turn out to be favored by the experimental data, they might have a fundamental reason and should originate from the underlying flavor theory. Hence a phenomenological study of possible texture zeros of M_ν *does* make a lot of sense.

As M_ν is symmetric, it has six independent complex entries. If n of them are taken to be

vanishing (i.e., M_ν has n independent texture zeros), then we shall arrive at

$${}^6\mathbf{C}_n = \frac{6!}{n!(6-n)!} \quad (1)$$

different textures. It is easy to show that a texture of M_ν with more than two independent zeros (i.e., $n \geq 3$) is definitely incompatible with current experimental data on neutrino masses and flavor mixing angles [9]. Hence a number of authors have paid particular interest to the two-zero textures of M_ν [10]—[14]¹. There are totally fifteen two-zero textures of M_ν , which can be classified into six categories:

$$\mathbf{A}_1 : \begin{pmatrix} 0 & 0 & \times \\ 0 & \times & \times \\ \times & \times & \times \end{pmatrix}, \quad \mathbf{A}_2 : \begin{pmatrix} 0 & \times & 0 \\ \times & \times & \times \\ 0 & \times & \times \end{pmatrix}; \quad (2)$$

$$\begin{aligned} \mathbf{B}_1 : \begin{pmatrix} \times & \times & 0 \\ \times & 0 & \times \\ 0 & \times & \times \end{pmatrix}, \quad \mathbf{B}_2 : \begin{pmatrix} \times & 0 & \times \\ 0 & \times & \times \\ \times & \times & 0 \end{pmatrix}, \\ \mathbf{B}_3 : \begin{pmatrix} \times & 0 & \times \\ 0 & 0 & \times \\ \times & \times & \times \end{pmatrix}, \quad \mathbf{B}_4 : \begin{pmatrix} \times & \times & 0 \\ \times & \times & \times \\ 0 & \times & 0 \end{pmatrix}; \end{aligned} \quad (3)$$

$$\mathbf{C} : \begin{pmatrix} \times & \times & \times \\ \times & 0 & \times \\ \times & \times & 0 \end{pmatrix}; \quad (4)$$

$$\mathbf{D}_1 : \begin{pmatrix} \times & \times & \times \\ \times & 0 & 0 \\ \times & 0 & \times \end{pmatrix}, \quad \mathbf{D}_2 : \begin{pmatrix} \times & \times & \times \\ \times & \times & 0 \\ \times & 0 & 0 \end{pmatrix}; \quad (5)$$

$$\mathbf{E}_1 : \begin{pmatrix} 0 & \times & \times \\ \times & 0 & \times \\ \times & \times & \times \end{pmatrix}, \quad \mathbf{E}_2 : \begin{pmatrix} 0 & \times & \times \\ \times & \times & \times \\ \times & \times & 0 \end{pmatrix}, \quad \mathbf{E}_3 : \begin{pmatrix} 0 & \times & \times \\ \times & \times & 0 \\ \times & 0 & \times \end{pmatrix}; \quad (6)$$

and

$$\mathbf{F}_1 : \begin{pmatrix} \times & 0 & 0 \\ 0 & \times & \times \\ 0 & \times & \times \end{pmatrix}, \quad \mathbf{F}_2 : \begin{pmatrix} \times & 0 & \times \\ 0 & \times & 0 \\ \times & 0 & \times \end{pmatrix}, \quad \mathbf{F}_3 : \begin{pmatrix} \times & \times & 0 \\ \times & \times & 0 \\ 0 & 0 & \times \end{pmatrix}, \quad (7)$$

in which each “ \times ” denotes a nonzero matrix element. Previous analyses of these fifteen patterns (see, e.g., Ref. [13]) led us to the following conclusions: (1) seven patterns (i.e., $\mathbf{A}_{1,2}$, $\mathbf{B}_{1,2,3,4}$

¹It is worth mentioning that the one-zero textures of M_ν have much less predictability than the two-zero textures of M_ν , and their phenomenological implications have been discussed in Ref. [15].

and **C**) were phenomenologically favored; (2) two patterns (i.e., **D**_{1,2}) were only marginally allowed; and (3) six patterns (i.e., **E**_{1,2,3} and **F**_{1,2,3}) were ruled out. Taking account of the latest T2K and MINOS neutrino oscillation data, one may wonder whether the above conclusions remain true or not. A fast check tells us that Patterns **D**_{1,2} can be ruled out by today's experimental data at the 3σ level, simply because $\theta_{12} > 38^\circ$ is no more favored. In addition, Patterns **E**_{1,2,3} and **F**_{1,2,3} remain phenomenologically disfavored. The question turns out to be whether Patterns **A**_{1,2}, **B**_{1,2,3,4} and **C** can survive current experimental tests and coincide with a relatively large value of θ_{13} . The main purpose of this paper is just to answer this question.

We aim to perform a very systematic study of the aforementioned seven patterns of M_ν with two independent texture zeros based on a global fit of current neutrino oscillation data done by Fogli *et al* [16]². Because a two-zero texture of M_ν is very simple and can reveal the salient phenomenological features of a given Majorana neutrino mass matrix, we intend to take such a systematic analysis as a good example to show how to test possible textures of M_ν by confronting them with more and more accurate experimental data. Hence this work is different from any of the previous ones. In particular, almost all the physical consequences of Patterns **A**_{1,2}, **B**_{1,2,3,4} and **C** are explored in an analytical way in the present work; the stability of texture zeros and the permutation symmetry between two similar patterns are discussed; the numerical analysis is most updated and more complete; and a realization of texture zeros by mean of certain flavor symmetries is illustrated. We find that Patterns **A**_{1,2}, **B**_{1,2,3,4} and **C** of M_ν can all survive current experimental tests at the 3σ level, but we believe that some of them are likely to be ruled out in the near future.

The remaining parts of this paper are organized as follows. In section 2 we show that the full neutrino mass spectrum and two Majorana CP-violating phases (ρ, σ) can all be determined in terms of three flavor mixing angles ($\theta_{12}, \theta_{23}, \theta_{13}$) and the Dirac CP-violating phase (δ) for a given two-zero texture of M_ν . Section 3 is devoted to a complete analytical analysis of Patterns **A**_{1,2}, **B**_{1,2,3,4} and **C** of M_ν , and to some discussions about the stability of texture zeros against the one-loop quantum corrections and the permutation symmetry between two similar patterns under consideration. With the help of current neutrino oscillation data we perform a detailed numerical analysis of those typical patterns of M_ν in section 4. Section 5 is devoted to some discussions about how to realize texture zeros of M_ν by means of certain flavor symmetries, and section 6 is a summary of this work together with some concluding remarks.

2 Basic Formulas

2.1 Important relations

In the flavor basis where the charged-lepton mass matrix M_l is diagonal, the Majorana neutrino mass matrix M_ν can be reconstructed in terms of three neutrino masses (m_1, m_2, m_3) and the

²Note that Schwetz *et al* have done another global fit of current data [17]. Although their best-fit results of three flavor mixing angles are slightly different from those obtained by Fogli *et al* [16], such differences become insignificant at the 3σ level. Therefore, we shall mainly use the 3σ results of [16] in our numerical calculations.

flavor mixing matrix V . Namely,

$$M_\nu = V \begin{pmatrix} m_1 & 0 & 0 \\ 0 & m_2 & 0 \\ 0 & 0 & m_3 \end{pmatrix} V^T. \quad (8)$$

It is convenient to express V as $V = UP$, where U denotes a 3×3 unitary matrix consisting of three flavor mixing angles $(\theta_{12}, \theta_{23}, \theta_{13})$ and one Dirac CP-violating phase (δ) , and $P = \text{Diag}\{e^{i\rho}, e^{i\sigma}, 1\}$ is a diagonal phase matrix containing two Majorana CP-violating phases (ρ, σ) . More explicitly, we adopt the parametrization

$$U = \begin{pmatrix} c_{12}c_{13} & s_{12}c_{13} & s_{13} \\ -c_{12}s_{23}s_{13} - s_{12}c_{23}e^{-i\delta} & -s_{12}s_{23}s_{13} + c_{12}c_{23}e^{-i\delta} & s_{23}c_{13} \\ -c_{12}c_{23}s_{13} + s_{12}s_{23}e^{-i\delta} & -s_{12}c_{23}s_{13} - c_{12}s_{23}e^{-i\delta} & c_{23}c_{13} \end{pmatrix}, \quad (9)$$

where $s_{ij} \equiv \sin \theta_{ij}$ and $c_{ij} \equiv \cos \theta_{ij}$ (for $ij = 12, 23, 13$) are defined. The neutrino mass matrix M_ν can equivalently be written as

$$M_\nu = U \begin{pmatrix} \lambda_1 & 0 & 0 \\ 0 & \lambda_2 & 0 \\ 0 & 0 & \lambda_3 \end{pmatrix} U^T, \quad (10)$$

where $\lambda_1 = m_1 e^{2i\rho}$, $\lambda_2 = m_2 e^{2i\sigma}$ and $\lambda_3 = m_3$. If two independent elements of M_ν are vanishing (i.e., $(M_\nu)_{ab} = (M_\nu)_{\alpha\beta} = 0$ with $ab \neq \alpha\beta$) as shown in Eqs. (2)–(7), one can obtain [11]

$$\begin{aligned} \frac{\lambda_1}{\lambda_3} &= \frac{U_{a3}U_{b3}U_{\alpha 2}U_{\beta 2} - U_{a2}U_{b2}U_{\alpha 3}U_{\beta 3}}{U_{a2}U_{b2}U_{\alpha 1}U_{\beta 1} - U_{a1}U_{b1}U_{\alpha 2}U_{\beta 2}}, \\ \frac{\lambda_2}{\lambda_3} &= \frac{U_{a1}U_{b1}U_{\alpha 3}U_{\beta 3} - U_{a3}U_{b3}U_{\alpha 1}U_{\beta 1}}{U_{a2}U_{b2}U_{\alpha 1}U_{\beta 1} - U_{a1}U_{b1}U_{\alpha 2}U_{\beta 2}}, \end{aligned} \quad (11)$$

from which two neutrino mass ratios are given by

$$\begin{aligned} \xi &\equiv \frac{m_1}{m_3} = \left| \frac{U_{a3}U_{b3}U_{\alpha 2}U_{\beta 2} - U_{a2}U_{b2}U_{\alpha 3}U_{\beta 3}}{U_{a2}U_{b2}U_{\alpha 1}U_{\beta 1} - U_{a1}U_{b1}U_{\alpha 2}U_{\beta 2}} \right|, \\ \zeta &\equiv \frac{m_2}{m_3} = \left| \frac{U_{a1}U_{b1}U_{\alpha 3}U_{\beta 3} - U_{a3}U_{b3}U_{\alpha 1}U_{\beta 1}}{U_{a2}U_{b2}U_{\alpha 1}U_{\beta 1} - U_{a1}U_{b1}U_{\alpha 2}U_{\beta 2}} \right|, \end{aligned} \quad (12)$$

and two Majorana CP-violating phases turn out to be

$$\begin{aligned} \rho &= \frac{1}{2} \arg \left[\frac{U_{a3}U_{b3}U_{\alpha 2}U_{\beta 2} - U_{a2}U_{b2}U_{\alpha 3}U_{\beta 3}}{U_{a2}U_{b2}U_{\alpha 1}U_{\beta 1} - U_{a1}U_{b1}U_{\alpha 2}U_{\beta 2}} \right], \\ \sigma &= \frac{1}{2} \arg \left[\frac{U_{a1}U_{b1}U_{\alpha 3}U_{\beta 3} - U_{a3}U_{b3}U_{\alpha 1}U_{\beta 1}}{U_{a2}U_{b2}U_{\alpha 1}U_{\beta 1} - U_{a1}U_{b1}U_{\alpha 2}U_{\beta 2}} \right]. \end{aligned} \quad (13)$$

2.2 Parameter counting

Since we have assumed massive neutrinos to be the Majorana particles, there are nine physical parameters: three neutrino masses (m_1, m_2, m_3) , three flavor mixing angles $(\theta_{12}, \theta_{23}, \theta_{13})$, and

three CP-violating phases (δ, ρ, σ) . By imposing two independent texture zeros on M_ν , we obtain four constraint relations as given in Eqs. (12) and (13). With the help of current experimental data on three flavor mixing angles and two independent neutrino mass-squared differences, defined as [16]

$$\delta m^2 \equiv m_2^2 - m_1^2, \quad \Delta m^2 = m_3^2 - \frac{1}{2}(m_1^2 + m_2^2), \quad (14)$$

one may determine or constrain both the neutrino mass spectrum and three CP-violating phases through Eqs. (12) and (13).

We take $(\theta_{12}, \theta_{23}, \theta_{13})$ and $(\delta m^2, \Delta m^2)$ as observables to see why the neutrino mass spectrum and three CP-violating phases can in principle be determined or constrained. First of all, note that $\xi = m_1/m_3$ and $\zeta = m_2/m_3$ are functions of the Dirac CP-violating phase δ as shown in Eq. (12). Then it is possible to determine or constrain δ from the relation

$$R_\nu \equiv \frac{\delta m^2}{|\Delta m^2|} = \frac{2(\zeta^2 - \xi^2)}{|2 - (\zeta^2 + \xi^2)|}. \quad (15)$$

Once δ is fixed, we can obtain (ξ, ζ) and (ρ, σ) from Eq. (12) and Eq. (13), respectively. In addition we have

$$m_3 = \frac{\sqrt{\delta m^2}}{\sqrt{\zeta^2 - \xi^2}}, \quad m_2 = m_3 \zeta, \quad m_1 = m_3 \xi. \quad (16)$$

Thus the neutrino mass spectrum is fully determined.

Table 1 shows the global-fit values of $(\theta_{12}, \theta_{23}, \theta_{13})$ and $(\delta m^2, \Delta m^2)$ obtained by assuming CP conservation with $\cos \delta = \pm 1$ [16]. We allow these parameters to independently vary in their 3σ ranges:

$$\begin{aligned} 0.259 \leq \sin^2 \theta_{12} \leq 0.359 & \quad \text{or} \quad 30.6^\circ \leq \theta_{12} \leq 36.8^\circ, \\ 0.340 \leq \sin^2 \theta_{23} \leq 0.640 & \quad \text{or} \quad 35.7^\circ \leq \theta_{23} \leq 53.1^\circ, \\ 0.001 \leq \sin^2 \theta_{13} \leq 0.044 & \quad \text{or} \quad 1.8^\circ \leq \theta_{13} \leq 12.1^\circ; \end{aligned} \quad (17)$$

and

$$\begin{aligned} 6.99 \times 10^{-5} \text{ eV}^2 \leq \delta m^2 \leq 8.18 \times 10^{-5} \text{ eV}^2, \\ 2.06 \times 10^{-3} \text{ eV}^2 \leq |\Delta m^2| \leq 2.67 \times 10^{-3} \text{ eV}^2. \end{aligned} \quad (18)$$

In our numerical calculations we shall treat δ as an unconstrained parameter. Note that the sign of Δm^2 remains unknown: $\Delta m^2 > 0$ or $\Delta m^2 < 0$ corresponds to the normal or inverted mass hierarchy of three neutrinos.

3 Two-zero Textures of M_ν

3.1 Stability of texture zeros

We first examine the stability of texture zeros of M_ν against the one-loop quantum corrections. To be explicit, we consider the unique dimension-5 Weinberg operator of massive Majorana

Table 1: The latest global-fit results of three neutrino mixing angles ($\theta_{12}, \theta_{23}, \theta_{13}$) and two neutrino mass-squared differences δm^2 and Δm^2 defined in Eq. (14). Here $\cos \delta = \pm 1$, and the old reactor antineutrino fluxes have been assumed [16].

Parameter	δm^2 (10^{-5} eV 2)	Δm^2 (10^{-3} eV 2)	θ_{12}	θ_{23}	θ_{13}
Best fit	7.58	2.35	33.6°	40.4°	8.3°
1 σ range	[7.32, 7.80]	[2.26, 2.47]	[32.6°, 34.7°]	[38.6°, 45.0°]	[6.5°, 9.6°]
2 σ range	[7.16, 7.99]	[2.17, 2.57]	[31.6°, 35.8°]	[36.9°, 50.8°]	[5.1°, 10.9°]
3 σ range	[6.99, 8.18]	[2.06, 2.67]	[30.6°, 36.8°]	[35.7°, 53.1°]	[1.8°, 12.1°]

neutrinos in an effective field theory after the heavy degrees of freedom are integrated out [18]:

$$\frac{\mathcal{L}_{d=5}}{\Lambda} = \frac{1}{2} \kappa_{\alpha\beta} \overline{\ell_{\alpha L}} \tilde{H} \tilde{H}^T \ell_{\beta L}^c + \text{h.c.} , \quad (19)$$

where Λ is the cutoff scale, ℓ_L denotes the left-handed lepton doublet, $\tilde{H} \equiv i\sigma_2 H^*$ with H being the standard-model Higgs doublet, and κ stands for the effective neutrino coupling matrix. After spontaneous gauge symmetry breaking, \tilde{H} gains its vacuum expectation value $\langle \tilde{H} \rangle = v/\sqrt{2}$ with $v \approx 246$ GeV. We are then left with the effective Majorana mass matrix $M_\nu = \kappa v^2/2$ for three light neutrinos from Eq. (19). If the dimension-5 Weinberg operator is obtained in the framework of the minimal supersymmetric standard model, one will be left with $M_\nu = \kappa(v \sin \beta)^2/2$, where $\tan \beta$ denotes the ratio of the vacuum expectation values of two Higgs doublets. Eq. (19) or its supersymmetric counterpart can provide a way of generating tiny neutrino masses. There are a number of interesting possibilities of building renormalizable gauge models to realize the effective Weinberg mass operator, such as the well-known seesaw mechanisms at a superhigh energy scale Λ [19, 20, 21].

The running of M_ν from Λ to the electroweak scale $\mu \simeq M_Z$ (or vice versa) is described by the renormalization-group equations (RGEs) [22]. In the chosen flavor basis and at the one-loop level, $M_\nu(M_Z)$ and $M_\nu(\Lambda)$ are related to each other via

$$M_\nu(M_Z) = I_0 \begin{pmatrix} I_e & 0 & 0 \\ 0 & I_\mu & 0 \\ 0 & 0 & I_\tau \end{pmatrix} M_\nu(\Lambda) \begin{pmatrix} I_e & 0 & 0 \\ 0 & I_\mu & 0 \\ 0 & 0 & I_\tau \end{pmatrix} , \quad (20)$$

where the RGE evolution function I_0 denotes the overall contribution from gauge and quark Yukawa couplings, and I_α (for $\alpha = e, \mu, \tau$) stand for the contributions from charged-lepton Yukawa couplings [23]. Because of $I_e < I_\mu < I_\tau$ as a consequence of $m_e \ll m_\mu \ll m_\tau$, they can modify the texture of M_ν . In comparison, $I_0 \neq 1$ only affects the overall mass scale of M_ν . Note, however, that the texture zeros of M_ν are stable against such quantum corrections induced by the one-loop RGEs. Taking Pattern \mathbf{A}_1 of M_ν for example, we have

$$M_\nu^{\mathbf{A}_1}(\Lambda) = \begin{pmatrix} 0 & 0 & a \\ 0 & b & c \\ a & c & d \end{pmatrix} \quad (21)$$

at Λ , and thus

$$M_\nu^{\mathbf{A}_1}(M_Z) = I_0 \begin{pmatrix} 0 & 0 & aI_e I_\tau \\ 0 & bI_\mu^2 & cI_\mu I_\tau \\ aI_e I_\tau & cI_\mu I_\tau & dI_\tau^2 \end{pmatrix} \quad (22)$$

at M_Z . This interesting feature implies that the important relations obtained in Eqs. (12) and (13) formally hold both at Λ and M_Z . In other words, if a seesaw or flavor symmetry model predicts a two-zero texture of M_ν at Λ , one may simply study its phenomenological consequences at M_Z by taking account of the same texture zeros. While the values of neutrino masses and flavor mixing parameters at M_Z turn out to be different from those at Λ , their correlations dictated by the texture zeros keep unchanged at any scale between Λ and M_Z .

3.2 Permutation symmetry

As pointed out in Refs. [10]—[14], the seven viable two-zero textures of M_ν can be classified into three distinct categories: (1) \mathbf{A}_1 and \mathbf{A}_2 ; (2) \mathbf{B}_1 , \mathbf{B}_2 , \mathbf{B}_3 and \mathbf{B}_4 ; and (3) \mathbf{C} . The phenomenological implications of those patterns in the same category have been found to be almost indistinguishable. Now we show that there exists a permutation symmetry between Patterns \mathbf{A}_1 and \mathbf{A}_2 , \mathbf{B}_1 and \mathbf{B}_2 , or \mathbf{B}_3 and \mathbf{B}_4 . This observation may help understand their similarities in model building and phenomenology.

Let us take Patterns \mathbf{A}_1 and \mathbf{A}_2 in Eq. (2) for example. Note that the location of texture zeros in \mathbf{A}_1 can be changed to that in \mathbf{A}_2 by a permutation in the 2-3 rows and 2-3 columns. To be explicit, we define the elementary transformation matrix

$$P_{23} = \begin{pmatrix} 1 & 0 & 0 \\ 0 & 0 & 1 \\ 0 & 1 & 0 \end{pmatrix}. \quad (23)$$

Then the Majorana neutrino mass matrix $M_\nu^{\mathbf{A}_2}$ can be constructed from $M_\nu^{\mathbf{A}_1}$ via

$$M_\nu^{\mathbf{A}_2} = P_{23} M_\nu^{\mathbf{A}_1} P_{23}^T. \quad (24)$$

If $M_\nu^{\mathbf{A}_1}$ is diagonalized by a unitary matrix $V = UP$ like Eq. (8), then Eq. (24) tells us that $M_\nu^{\mathbf{A}_2}$ can be diagonalized by the unitary matrix $\tilde{V} = \tilde{U}P$ with $\tilde{U} = P_{23}U$. Parametrizing \tilde{U} in terms of three rotation angles $(\tilde{\theta}_{12}, \tilde{\theta}_{23}, \tilde{\theta}_{13})$ and one CP-violating phase $\tilde{\delta}$, just like the parametrization of U in Eq. (9), we immediately obtain the relations

$$\tilde{\theta}_{12} = \theta_{12}, \quad \tilde{\theta}_{13} = \theta_{13}, \quad \tilde{\theta}_{23} = \frac{\pi}{2} - \theta_{23}, \quad \tilde{\delta} = \delta - \pi. \quad (25)$$

In addition, $M_\nu^{\mathbf{A}_1}$ and $M_\nu^{\mathbf{A}_2}$ have the same eigenvalues λ_i (for $i = 1, 2, 3$). The phenomenological predictions of Pattern \mathbf{A}_2 can therefore be obtained from those of Pattern \mathbf{A}_1 by implementing the replacements in Eq. (25). It is easy to show that a similar permutation symmetry holds between Patterns \mathbf{B}_1 and \mathbf{B}_2 or between Patterns \mathbf{B}_3 and \mathbf{B}_4 .

3.3 Analytical approximations

Thanks to the permutation symmetry discussed above, it is only necessary to study Patterns \mathbf{A}_1 , \mathbf{B}_1 , \mathbf{B}_3 and \mathbf{C} in detail. The analytical results for \mathbf{A}_2 , \mathbf{B}_2 and \mathbf{B}_4 can be obtained, respectively, from those for \mathbf{A}_1 , \mathbf{B}_1 and \mathbf{B}_3 with the replacements $\theta_{23} \rightarrow \pi/2 - \theta_{23}$ and $\delta \rightarrow \delta - \pi$. In this subsection we explore the analytical relations among three neutrino masses (m_1, m_2, m_3) , three flavor mixing angles $(\theta_{12}, \theta_{23}, \theta_{13})$ and three CP-violating phases (δ, ρ, σ) for each pattern of M_ν by means of Eqs. (11)–(16). The effective mass term of the neutrinoless double-beta decay, defined as $\langle m \rangle_{ee} \equiv |(M_\nu)_{ee}|$, will also be discussed.

- **Pattern \mathbf{A}_1** with $(M_\nu)_{ee} = (M_\nu)_{e\mu} = 0$. With the help of Eq. (11), we obtain [11]

$$\begin{aligned} \frac{\lambda_1}{\lambda_3} &= +\frac{s_{13}}{c_{13}^2} \left(\frac{s_{12}s_{23}}{c_{12}c_{23}} e^{i\delta} - s_{13} \right), \\ \frac{\lambda_2}{\lambda_3} &= -\frac{s_{13}}{c_{13}^2} \left(\frac{c_{12}s_{23}}{s_{12}c_{23}} e^{i\delta} + s_{13} \right). \end{aligned} \quad (26)$$

Since $s_{13}^2 \ll 1$ is a good approximation, Eq. (26) immediately leads us to the results

$$\begin{aligned} \xi = \frac{m_1}{m_3} &\approx \tan \theta_{12} \tan \theta_{23} \sin \theta_{13}, \\ \zeta = \frac{m_2}{m_3} &\approx \cot \theta_{12} \tan \theta_{23} \sin \theta_{13}; \end{aligned} \quad (27)$$

and

$$\begin{aligned} \rho &\approx \frac{\delta}{2}, \\ \sigma &\approx \frac{\delta}{2} - \frac{\pi}{2}. \end{aligned} \quad (28)$$

Without loss of generality, we choose three neutrino mixing angles to lie in the first quadrant and allow three CP-violating phases to vary in the ranges $\rho \in [-\pi/2, +\pi/2]$, $\sigma \in [-\pi/2, +\pi/2]$ and $\delta \in [0, 2\pi]$. Given $0.60 \leq \tan \theta_{12} \leq 0.75$, $0.72 \leq \tan \theta_{23} \leq 1.3$ and $0.03 \leq \sin \theta_{13} \leq 0.21$ at the 3σ level, Eq. (27) yields $\xi < \zeta < 1$. So the normal neutrino mass hierarchy $m_1 < m_2 < m_3$ follows and $\Delta m^2 > 0$ holds. As indicated by Eq. (15), the Dirac CP-violating phase δ can completely be fixed if three neutrino mixing angles and two neutrino mass-squared differences are known. In the lowest order of s_{13} , however,

$$R_\nu = \frac{\delta m^2}{\Delta m^2} \approx \frac{4 \tan^2 \theta_{23} \sin^2 \theta_{13}}{\sin 2\theta_{12} \tan 2\theta_{12}}, \quad (29)$$

which is actually independent of δ . So we have to go beyond the leading order approximation. To the next-to-leading order we obtain

$$\begin{aligned} \xi = \frac{m_1}{m_3} &\approx \tan \theta_{12} \tan \theta_{23} \sin \theta_{13} \sqrt{1 - 2 \cot \theta_{12} \cot \theta_{23} \sin \theta_{13} \cos \delta}, \\ \zeta = \frac{m_2}{m_3} &\approx \cot \theta_{12} \tan \theta_{23} \sin \theta_{13} \sqrt{1 + 2 \tan \theta_{12} \cot \theta_{23} \sin \theta_{13} \cos \delta}; \end{aligned} \quad (30)$$

and

$$R_\nu \approx \zeta^2 - \xi^2 = \frac{4 \tan^2 \theta_{23} \sin^2 \theta_{13}}{\sin 2\theta_{12} \tan 2\theta_{12}} (1 + \tan 2\theta_{12} \cot \theta_{23} \sin \theta_{13} \cos \delta) . \quad (31)$$

Finally we arrive at

$$\delta \approx \cos^{-1} \left[+ \frac{\tan \theta_{23}}{\tan 2\theta_{12} \sin \theta_{13}} \left(\frac{\sin 2\theta_{12} \tan 2\theta_{12} R_\nu}{4 \tan^2 \theta_{23} \sin^2 \theta_{13}} - 1 \right) \right] . \quad (32)$$

Taking the best-fit values of the three neutrino mixing angles (i.e., $\theta_{12} = 33.6^\circ$, $\theta_{23} = 40.4^\circ$ and $\theta_{13} = 8.3^\circ$) together with those of two neutrino mass-squared differences (i.e., $\delta m^2 = 7.58 \times 10^{-5} \text{ eV}^2$ and $\Delta m^2 = 2.35 \times 10^{-3} \text{ eV}^2$) from Table 1, one immediately obtains the neutrino mass spectrum ³

$$\begin{aligned} m_3 &\approx \sqrt{\Delta m^2} = 4.8 \times 10^{-2} \text{ eV} , \\ m_2 &\approx m_3 \cot \theta_{12} \tan \theta_{23} \sin \theta_{13} = 8.9 \times 10^{-3} \text{ eV} , \\ m_1 &\approx m_3 \tan \theta_{12} \tan \theta_{23} \sin \theta_{13} = 3.9 \times 10^{-3} \text{ eV} ; \end{aligned} \quad (33)$$

and the CP-violating phases $\delta \approx 64^\circ$, $\rho \approx 32^\circ$ and $\sigma \approx -58^\circ$. Since $(M_\nu)_{ee} = 0$ holds for Pattern **A₁** of M_ν , the effective mass $\langle m \rangle_{ee}$ of the neutrinoless double-beta decay is definitely vanishing.

- **Pattern A₂** with $(M_\nu)_{ee} = (M_\nu)_{e\tau} = 0$. As pointed out in section 3.2, all the analytical results of Pattern **A₂** can be obtained from those of Pattern **A₁** with the replacements $\theta_{23} \rightarrow \pi/2 - \theta_{23}$ and $\delta \rightarrow \delta - \pi$. So it is straightforward to have

$$\begin{aligned} \xi = \frac{m_1}{m_3} &\approx \tan \theta_{12} \cot \theta_{23} \sin \theta_{13} \sqrt{1 + 2 \cot \theta_{12} \tan \theta_{23} \sin \theta_{13} \cos \delta} , \\ \zeta = \frac{m_2}{m_3} &\approx \cot \theta_{12} \cot \theta_{23} \sin \theta_{13} \sqrt{1 - 2 \tan \theta_{12} \tan \theta_{23} \sin \theta_{13} \cos \delta} ; \end{aligned} \quad (34)$$

and

$$\delta \approx \cos^{-1} \left[- \frac{\cot \theta_{23}}{\tan 2\theta_{12} \sin \theta_{13}} \left(\frac{\sin 2\theta_{12} \tan 2\theta_{12} R_\nu}{4 \cot^2 \theta_{23} \sin^2 \theta_{13}} - 1 \right) \right] . \quad (35)$$

In addition,

$$\begin{aligned} \rho &\approx \frac{\delta}{2} - \frac{\pi}{2} , \\ \sigma &\approx \frac{\delta}{2} ; \end{aligned} \quad (36)$$

and the neutrino mass spectrum turns out to be

$$\begin{aligned} m_3 &\approx \sqrt{\Delta m^2} , \\ m_2 &\approx m_3 \cot \theta_{12} \cot \theta_{23} \sin \theta_{13} , \\ m_1 &\approx m_3 \tan \theta_{12} \cot \theta_{23} \sin \theta_{13} . \end{aligned} \quad (37)$$

³Note again that such best-fit values have been obtained in the assumption of $\cos \delta = \pm 1$ [16]. To give a rough estimate, however, we assume that they are essentially unchanged even for an arbitrary value of δ .

Similar to the case of Pattern \mathbf{A}_1 , $\langle m \rangle_{ee} = |(M_\nu)_{ee}| = 0$ holds in Pattern \mathbf{A}_2 . Provided the same best-fit values of δm^2 , Δm^2 , θ_{12} , θ_{23} and θ_{13} are taken, one can easily verify that $\cos \delta > 1$ holds, implying a potential inconsistency of Pattern \mathbf{A}_2 with current experimental data. When the uncertainties of those neutrino mixing parameters are taken into account (e.g., at the 3σ level), however, we actually find no problem with Pattern \mathbf{A}_2 (see the numerical analysis in section 4).

- **Pattern \mathbf{B}_1** with $(M_\nu)_{\mu\mu} = (M_\nu)_{e\tau} = 0$. With the help of Eq. (11), we obtain

$$\begin{aligned} \frac{\lambda_1}{\lambda_3} &= \frac{s_{12}c_{12}s_{23}(2c_{23}^2s_{13}^2 - s_{23}^2c_{13}^2) - c_{23}s_{13}(s_{12}^2s_{23}^2e^{+i\delta} + c_{12}^2c_{23}^2e^{-i\delta})}{s_{12}c_{12}s_{23}c_{23}^2 + (s_{12}^2 - c_{12}^2)c_{23}^3s_{13}e^{i\delta} + s_{12}c_{12}s_{23}s_{13}^2(1 + c_{23}^2)e^{2i\delta}}e^{2i\delta}, \\ \frac{\lambda_2}{\lambda_3} &= \frac{s_{12}c_{12}s_{23}(2c_{23}^2s_{13}^2 - s_{23}^2c_{13}^2) + c_{23}s_{13}(c_{12}^2s_{23}^2e^{+i\delta} + s_{12}^2c_{23}^2e^{-i\delta})}{s_{12}c_{12}s_{23}c_{23}^2 + (s_{12}^2 - c_{12}^2)c_{23}^3s_{13}e^{i\delta} + s_{12}c_{12}s_{23}s_{13}^2(1 + c_{23}^2)e^{2i\delta}}e^{2i\delta}. \end{aligned} \quad (38)$$

In the leading order approximation,

$$\begin{aligned} \xi &= \frac{m_1}{m_3} \approx \tan^2 \theta_{23}, \\ \zeta &= \frac{m_2}{m_3} \approx \tan^2 \theta_{23}; \end{aligned} \quad (39)$$

and

$$\rho \approx \sigma \approx \delta - \frac{\pi}{2}. \quad (40)$$

In the next-to-leading order approximation, we find

$$\begin{aligned} \frac{m_1}{m_3} - \frac{m_2}{m_3} &\approx + \frac{4 \sin \theta_{13} \cos \delta}{\sin 2\theta_{12} \sin 2\theta_{23}}, \\ \rho - \sigma &\approx - \frac{2 \sin \theta_{13} \sin \delta}{\sin 2\theta_{12} \tan 2\theta_{23} \tan^2 \theta_{23}}. \end{aligned} \quad (41)$$

The Dirac CP-violating phase δ can be determined from

$$R_\nu \approx \frac{2 \sin \theta_{13}}{\sin 2\theta_{12}} |\tan 2\theta_{23} \cos \delta|. \quad (42)$$

Since $\delta m^2 > 0$ or equivalently $m_2 > m_1$, we have $\cos \delta < 0$ from Eq. (41). Taking the best-fit values, one can obtain $\delta \approx 91^\circ$ and thus $\rho \approx \sigma \approx 1^\circ$. Eq. (41) tells us that the difference between m_2/m_3 and m_1/m_3 is about 0.01, and that between ρ and σ is about 4° . On the other hand, the neutrino mass spectrum is given by

$$\begin{aligned} m_3 &\approx \sqrt{\frac{\Delta m^2}{1 - \tan^4 \theta_{23}}} \approx 7.0 \times 10^{-2} \text{ eV}, \\ m_2 &\approx m_1 \approx m_3 \tan^2 \theta_{23} \approx 5.1 \times 10^{-2} \text{ eV}; \end{aligned} \quad (43)$$

and the effective mass term of the neutrinoless double-beta decay turns out to be $\langle m \rangle_{ee} \approx m_3 \tan^2 \theta_{23} \approx 5.1 \times 10^{-2} \text{ eV}$. Note that we have input the best-fit value $\theta_{23} = 40.4^\circ$ [16],

so the normal neutrino mass hierarchy $m_3 > m_2 > m_1$ is allowed. If the 3σ range of θ_{23} is taken, however, both normal and inverted mass hierarchies are likely. When $\tan \theta_{23} > 1$, which is allowed at the 2σ or 3σ level [16], we have the inverted neutrino mass hierarchy with $\Delta m^2 < 0$. In short, the analytical formulas for m_1 , m_2 and m_3 in Eq. (43) are valid no matter which mass hierarchy is taken, but the corresponding numerical results depend on the input value of θ_{23} .

- **Pattern \mathbf{B}_2** with $(M_\nu)_{\tau\tau} = (M_\nu)_{e\mu} = 0$. By using the permutation symmetry discussed in section 3.2, we obtain

$$\begin{aligned}\xi &= \frac{m_1}{m_3} \approx \cot^2 \theta_{23}, \\ \zeta &= \frac{m_2}{m_3} \approx \cot^2 \theta_{23};\end{aligned}\tag{44}$$

and

$$\rho \approx \sigma \approx \delta - \frac{\pi}{2}\tag{45}$$

in the leading order approximation. Note that there is a period of π for ρ and σ , so Eq. (45) is identical to Eq. (40) even if the replacement $\delta \rightarrow \delta - \pi$ is made. In the next-to-leading order approximation, we have

$$\begin{aligned}\frac{m_1}{m_3} - \frac{m_2}{m_3} &\approx -\frac{4 \sin \theta_{13} \cos \delta}{\sin 2\theta_{12} \sin 2\theta_{23}}, \\ \rho - \sigma &\approx -\frac{2 \sin \theta_{13} \sin \delta}{\sin 2\theta_{12} \tan 2\theta_{23} \cot^2 \theta_{23}}.\end{aligned}\tag{46}$$

The Dirac CP-violating phase is also determined by Eq. (42), because $|\tan 2\theta_{23}|$ keeps invariant under the replacement $\theta_{23} \rightarrow \pi/2 - \theta_{23}$. Now we have $\cos \delta > 0$ in view of the fact of $m_2 > m_1$. So $\delta \approx 89^\circ$ and $\rho \approx \sigma \approx -1^\circ$. Eq. (46) tells us that the difference between m_2/m_3 and m_1/m_3 is about 0.01, and that between ρ and σ is about 2° . The neutrino mass spectrum turns out to be

$$\begin{aligned}m_3 &\approx \sqrt{\frac{\Delta m^2}{1 - \cot^4 \theta_{23}}} \approx 5.1 \times 10^{-2} \text{ eV}, \\ m_2 &\approx m_1 \approx m_3 \cot^2 \theta_{23} \approx 7.0 \times 10^{-2} \text{ eV}.\end{aligned}\tag{47}$$

In addition, $\langle m \rangle_{ee} \approx m_3 \cot^2 \theta_{23} \approx 7.0 \times 10^{-2} \text{ eV}$. Note that we have input the best-fit value $\theta_{23} = 40.4^\circ$ [16], so the inverted mass hierarchy $m_2 > m_1 > m_3$ appears. If the 3σ range of θ_{23} is taken, however, both normal and inverted mass hierarchies are likely. Hence it is experimentally important to determine the deviation of θ_{23} from $\pi/4$.

- **Pattern \mathbf{B}_3** with $(M_\nu)_{\mu\mu} = (M_\nu)_{e\mu} = 0$. With the help of Eq. (11), we obtain

$$\begin{aligned}\frac{\lambda_1}{\lambda_3} &= -\frac{s_{23}}{c_{23}} \cdot \frac{s_{12}s_{23} - c_{12}c_{23}s_{13}e^{-i\delta}}{s_{12}c_{23} + c_{12}s_{23}s_{13}e^{+i\delta}} e^{2i\delta}, \\ \frac{\lambda_2}{\lambda_3} &= -\frac{s_{23}}{c_{23}} \cdot \frac{c_{12}s_{23} + s_{12}c_{23}s_{13}e^{-i\delta}}{c_{12}c_{23} - s_{12}s_{23}s_{13}e^{+i\delta}} e^{2i\delta}.\end{aligned}\tag{48}$$

In the leading order approximation,

$$\begin{aligned}\xi &= \frac{m_1}{m_3} \approx \tan^2 \theta_{23} , \\ \zeta &= \frac{m_2}{m_3} \approx \tan^2 \theta_{23} ;\end{aligned}\tag{49}$$

and

$$\rho \approx \sigma \approx \delta - \frac{\pi}{2} .\tag{50}$$

In the next-to-leading order approximation, we have

$$\begin{aligned}\frac{m_1}{m_3} - \frac{m_2}{m_3} &\approx -\frac{4 \tan^2 \theta_{23} \sin \theta_{13} \cos \delta}{\sin 2\theta_{12} \sin 2\theta_{23}} , \\ \rho - \sigma &\approx +\frac{2 \sin \theta_{13} \sin \delta}{\sin 2\theta_{12} \tan 2\theta_{23}} .\end{aligned}\tag{51}$$

The Dirac CP-violating phase δ can be determined from

$$R_\nu \approx \frac{2 \sin \theta_{13}}{\sin 2\theta_{12}} \tan^2 \theta_{23} |\tan 2\theta_{23} \cos \delta| .\tag{52}$$

The condition $m_2 > m_1$ leads to $\cos \delta > 0$. Taking the best-fit values [16], we obtain $\delta \approx 89^\circ$ and $\rho \approx \sigma \approx -1^\circ$ from Eq. (51). The difference between m_2/m_3 and m_1/m_3 is about 0.008, and that between ρ and σ is about 3° . On the other hand, the neutrino mass spectrum is given by

$$\begin{aligned}m_3 &\approx \sqrt{\frac{\Delta m^2}{1 - \tan^4 \theta_{23}}} \approx 7.0 \times 10^{-2} \text{ eV} , \\ m_2 &\approx m_1 \approx m_3 \tan^2 \theta_{23} \approx 5.1 \times 10^{-2} \text{ eV} .\end{aligned}\tag{53}$$

The effective mass term of the neutrinoless double-beta decay turns out to be $\langle m \rangle_{ee} \approx m_3 \tan^2 \theta_{23} \approx 5.1 \times 10^{-2} \text{ eV}$. Note that the phenomenology of Pattern \mathbf{B}_3 is essentially the same as that of Pattern \mathbf{B}_1 except for the Dirac CP-violating phase δ . Note also that we have used the best-fit value $\theta_{23} = 40.4^\circ$ [16], so the normal neutrino mass hierarchy $m_3 > m_2 > m_1$ is allowed. If the 3σ range of θ_{23} is taken, however, both normal and inverted neutrino mass hierarchies are likely.

- **Pattern \mathbf{B}_4** with $(M_\nu)_{\tau\tau} = (M_\nu)_{e\tau} = 0$. By using the permutation symmetry discussed in section 3.2, we obtain

$$\begin{aligned}\xi &= \frac{m_1}{m_3} \approx \cot^2 \theta_{23} , \\ \zeta &= \frac{m_2}{m_3} \approx \cot^2 \theta_{23} ;\end{aligned}\tag{54}$$

and

$$\rho \approx \sigma \approx \delta - \frac{\pi}{2}\tag{55}$$

in the leading order approximation. More accurately, we have

$$\begin{aligned}\frac{m_1}{m_3} - \frac{m_2}{m_3} &\approx + \frac{4 \cot^2 \theta_{23} \sin \theta_{13} \cos \delta}{\sin 2\theta_{12} \sin 2\theta_{23}}, \\ \rho - \sigma &\approx + \frac{2 \sin \theta_{13} \sin \delta}{\sin 2\theta_{12} \tan 2\theta_{23}}.\end{aligned}\quad (56)$$

The Dirac CP-violating phase is given by

$$R_\nu \approx \frac{2 \sin \theta_{13}}{\sin 2\theta_{12}} \cot^2 \theta_{23} |\tan 2\theta_{23} \cos \delta|. \quad (57)$$

We find $\cos \delta < 0$ from the fact of $m_2 > m_1$. Hence $\delta \approx 91^\circ$ and $\rho \approx \sigma \approx 1^\circ$. Eq. (56) tells us that the difference between m_2/m_3 and m_1/m_3 is about 0.015, and that between ρ and σ is about 3° . The neutrino mass spectrum turns out to be

$$\begin{aligned}m_3 &\approx \sqrt{\frac{\Delta m^2}{1 - \cot^4 \theta_{23}}} \approx 5.1 \times 10^{-2} \text{ eV}, \\ m_2 &\approx m_1 \approx m_3 \cot^2 \theta_{23} \approx 7.0 \times 10^{-2} \text{ eV}.\end{aligned}\quad (58)$$

In addition, $\langle m \rangle_{ee} \approx m_3 \cot^2 \theta_{23} \approx 7.0 \times 10^{-2} \text{ eV}$. Note that we have used the best-fit value $\theta_{23} = 40.4^\circ$ [16], so the inverted neutrino mass hierarchy $m_2 > m_1 > m_3$ appears. If the 3σ range of θ_{23} is taken, however, both normal and inverted mass hierarchies are likely. It is obvious that a precise determination of δ and the neutrino mass hierarchy is crucial to pin down one of the four patterns \mathbf{B}_1 , \mathbf{B}_2 , \mathbf{B}_3 and \mathbf{B}_4 . All of them predict a nearly degenerate neutrino mass spectrum.

- **Pattern C** with $(M_\nu)_{\mu\mu} = (M_\nu)_{\tau\tau} = 0$. With the help of Eq. (11), we obtain

$$\begin{aligned}\frac{\lambda_1}{\lambda_3} &= \frac{c_{12}c_{13}^2}{s_{13}} \cdot \frac{-c_{12}(s_{23}^2 - c_{23}^2) - 2s_{12}s_{23}c_{23}s_{13}e^{i\delta}}{2s_{12}c_{12}s_{23}c_{23} - (s_{12}^2 - c_{12}^2)(s_{23}^2 - c_{23}^2)s_{13}e^{i\delta} + 2s_{12}c_{12}s_{23}c_{23}s_{13}^2e^{2i\delta}} e^{i\delta}, \\ \frac{\lambda_2}{\lambda_3} &= \frac{s_{12}c_{13}^2}{s_{13}} \cdot \frac{+s_{12}(s_{23}^2 - c_{23}^2) - 2c_{12}s_{23}c_{23}s_{13}e^{i\delta}}{2s_{12}c_{12}s_{23}c_{23} - (s_{12}^2 - c_{12}^2)(s_{23}^2 - c_{23}^2)s_{13}e^{i\delta} + 2s_{12}c_{12}s_{23}c_{23}s_{13}^2e^{2i\delta}} e^{i\delta}.\end{aligned}\quad (59)$$

To the lowest order,

$$\begin{aligned}\xi = \frac{m_1}{m_3} &\approx \sqrt{1 - \frac{2 \cot \theta_{12} \cos \delta}{\tan 2\theta_{23} \sin \theta_{13}} + \frac{\cot^2 \theta_{12}}{\tan^2 2\theta_{23} \sin^2 \theta_{13}}}, \\ \zeta = \frac{m_2}{m_3} &\approx \sqrt{1 + \frac{2 \tan \theta_{12} \cos \delta}{\tan 2\theta_{23} \sin \theta_{13}} + \frac{\tan^2 \theta_{12}}{\tan^2 2\theta_{23} \sin^2 \theta_{13}}}.\end{aligned}\quad (60)$$

Since $m_2 > m_1$, Eq. (60) implies $\tan 2\theta_{23} \cos \delta > 0$ and $m_2 > m_3$. Furthermore, one can verify that $\tan 2\theta_{12} \tan 2\theta_{23} \sin \theta_{13} \cos \delta > 1$ is required to guarantee $m_2 > m_1$. Hence only the inverted mass hierarchy $m_2 > m_1 > m_3$ is allowed. The Dirac CP-violating phase δ can be determined from

$$R_\nu \approx \frac{2(1 + \tan \theta_{12} \tan \theta_{23})(\tan 2\theta_{12} \tan 2\theta_{23} \sin \theta_{13} \cos \delta - 1)}{\tan \theta_{12} \tan \theta_{23} \tan 2\theta_{12} (\tan \theta_{12} + 2 \tan 2\theta_{23} \sin \theta_{13} \cos \delta)}.\quad (61)$$

Taking the best-fit values of three neutrino mixing angles and two neutrino mass-squared differences, we obtain $\delta \approx 61^\circ$ from Eq. (61). The Majorana CP-violating phases ρ and σ turn out to be

$$\begin{aligned}\rho &\approx \delta + \frac{1}{2} \tan^{-1} \left[\frac{\cot \theta_{12} \sin \delta}{\tan 2\theta_{23} \sin \theta_{13} - \cot \theta_{12} \cos \delta} \right] - \frac{\pi}{2} \approx +13^\circ, \\ \sigma &\approx \delta - \frac{1}{2} \tan^{-1} \left[\frac{\tan \theta_{12} \sin \delta}{\tan 2\theta_{23} \sin \theta_{13} + \tan \theta_{12} \cos \delta} \right] - \frac{\pi}{2} \approx -42^\circ.\end{aligned}\quad (62)$$

Finally we obtain

$$\begin{aligned}m_3 &\approx \sqrt{\frac{\tan^2 2\theta_{23} \cot^2 \theta_{12} \sin^2 \theta_{13} \Delta m^2}{1 + 2 \cot \theta_{12} \tan 2\theta_{23} \sin \theta_{13} \cos \delta}} \approx 4.3 \times 10^{-2} \text{ eV}, \\ m_2 &\approx m_3 \sqrt{1 + \frac{2 \tan \theta_{12} \cos \delta}{\tan 2\theta_{23} \sin \theta_{13}} + \frac{\tan^2 \theta_{12}}{\tan^2 2\theta_{23} \sin^2 \theta_{13}}} \approx 6.6 \times 10^{-2} \text{ eV}, \\ m_1 &\approx m_3 \sqrt{1 - \frac{2 \cot \theta_{12} \cos \delta}{\tan 2\theta_{23} \sin \theta_{13}} + \frac{\cot^2 \theta_{12}}{\tan^2 2\theta_{23} \sin^2 \theta_{13}}} \approx 6.5 \times 10^{-2} \text{ eV}\end{aligned}\quad (63)$$

together with

$$\langle m \rangle_{ee} \approx m_3 \sqrt{1 - \frac{4 \cot 2\theta_{12} \cos \delta}{\tan 2\theta_{23} \sin \theta_{13}} + \frac{4 \cot^2 2\theta_{12}}{\tan^2 2\theta_{23} \sin^2 \theta_{13}}} \approx 4.1 \times 10^{-2} \text{ eV}.\quad (64)$$

Note that both $\tan 2\theta_{23} > 0$ with $\cos \delta > 0$ and $\tan 2\theta_{23} < 0$ with $\cos \delta < 0$ are likely, if the 3σ range of θ_{23} is taken into account. Nevertheless, the inverted mass hierarchy $m_3 < m_1 < m_2$ is expected in both cases. Going beyond the above analytical approximation, we find that the normal mass hierarchy $m_1 < m_2 < m_3$ is actually allowed if and only if θ_{23} lies in the vicinity of 45° ⁴. This point can be understood in a simple way. With the help of Eq. (59), one obtains

$$\frac{\lambda_1}{\lambda_3} = \frac{\lambda_2}{\lambda_3} = -\frac{c_{13}^2 e^{2i\delta}}{1 + s_{13}^2 e^{2i\delta}} \approx -c_{13}^2 e^{2i\delta} (1 - s_{13}^2 e^{2i\delta})\quad (65)$$

in the limit of $\theta_{23} = 45^\circ$, implying the mass hierarchy $m_1 = m_2 < m_3$ for $\theta_{13} \neq 0^\circ$. Hence a tiny deviation of θ_{23} from 45° is required to lift the degeneracy of m_1 and m_2 and then reproduce the small but nonvanishing value of R_ν , such that $m_1 < m_2 < m_3$ comes out. Because the parameter space of this possibility is too small, we shall mainly concentrate on the inverted mass hierarchy in our subsequent numerical analysis.

In summary, the analytical results for the three CP-violating phases (δ, ρ, σ) , the two neutrino mass ratios m_1/m_3 and m_2/m_3 , the absolute neutrino mass m_3 and the effective neutrino mass $\langle m \rangle_{ee}$, predicted by seven two-zero textures of M_ν , are listed in Tables 2–4. If the best-fit values of neutrino mixing parameters [16] are taken, we find that only Pattern **A**₂ can be excluded. We expect that all the seven patterns of M_ν can survive current experimental tests at the 3σ level. A detailed numerical analysis will be done in section 4.

⁴We thank the anonymous referee for pointing out this interesting possibility to us.

4 Numerical Analysis

The analytical results obtained above show that the neutrino mass hierarchy is actually related to the flavor mixing angle θ_{23} in Patterns \mathbf{B}_1 , \mathbf{B}_2 , \mathbf{B}_3 and \mathbf{B}_4 of M_ν . In particular, it depends on whether $\theta_{23} > 45^\circ$ or $\theta_{23} < 45^\circ$. According to Table 1 [16], only $\theta_{23} \leq 45^\circ$ is allowed at the 1σ level ⁵. If a two-zero texture of M_ν can accommodate both normal and inverted mass hierarchies, we shall only concentrate on the one dictated by $\theta_{23} < 45^\circ$ in our numerical analysis, because the other possibility is just an opposite and trivial exercise. We have noticed that the Dirac CP-violating phase δ should be close to $\pi/2$ or $3\pi/2$ in Patterns $\mathbf{B}_{1,2,3,4}$, and the differences between two Majorana CP-violating phases ρ and σ in these two cases are distinct. For illustration, we shall only focus on the range of δ around $\pi/2$ in our numerical analysis of these four patterns. The explicit calculations are done in the following way:

1. For each of the seven patterns of M_ν , we generate a set of random numbers of $(\theta_{12}, \theta_{23}, \theta_{13})$ and $(\delta m^2, \Delta m^2)$ lying in their 3σ ranges given by Eqs. (17) and (18) together with a random value of δ in the range $\delta \in [0, 2\pi]$.
2. Given the above random numbers, it is possible to calculate other physical parameters of M_ν , including three neutrino mass eigenvalues (m_1, m_2, m_3) , two Majorana-type CP-violating phases (ρ, σ) , the effective mass of the neutrinoless double-beta decay $\langle m \rangle_{ee}$ and the Jarlskog invariant of leptonic CP violation $J_{\text{CP}} = s_{12}c_{12}s_{23}c_{23}s_{13}c_{13}^2 \sin \delta$. To judge whether a pattern of M_ν is consistent with current experimental data or not, we require that the consistency conditions should be satisfied: (a) because of $\delta m^2 > 0$, we require $m_2 > m_1$ or equivalently $\zeta^2 - \xi^2 > 0$; (b) since only the neutrino mass hierarchies $m_2 > m_1 > m_3$ and $m_3 > m_2 > m_1$ are phenomenologically allowed, we further require $(\zeta^2 - 1)(\xi^2 - 1) > 0$ (i.e., $\xi^2 > 1$ and $\zeta^2 > 1$ correspond to the inverted mass hierarchy, whereas $\xi^2 < 1$ and $\zeta^2 < 1$ stand for the normal mass hierarchy); (c) given the values of three neutrino mixing angles and two mass-squared differences, the Dirac CP-violating phase δ is actually fixed by Eq. (15). Instead of solving δ , we require that Eq. (15) should be satisfied up to a reasonable degree of precision (e.g., 10^{-4}).
3. We consider all the points satisfying the consistency conditions, and then have a nine-dimensional parameter space spanned by nine quantities $(\theta_{12}, \theta_{23}, \theta_{13}, \delta, \rho, \sigma, m_1, m_2, m_3)$. The low-energy observables such as J_{CP} and $\langle m \rangle_{ee}$ can accordingly be calculated. To present the final results in a simple and clear way, we restrict ourselves to the two-dimensional parameter space and set the x -axis to be the Dirac CP-violating phase δ . Therefore, what we actually show are the allowed ranges of relevant physical parameters of each pattern of M_ν .
4. Corresponding to the allowed ranges of θ_{12} , θ_{23} and θ_{13} changing with δ , their histograms are also plotted because they can signify the most probable values of three flavor mixing

⁵Note that $\theta_{23} \geq 45^\circ$ seems to be favored at the 1σ level in the global analysis done by Schwetz *et al* [17].

angles. The height of each histogram indicates the number of points in each bin. Since the future neutrino oscillation experiments will greatly improve the measurements of three neutrino mixing angles, such a presentation should be helpful in judging which two-zero pattern of M_ν is phenomenologically more favored.

We stress that the strategy of our numerical analysis can also apply to other textures of the Majorana neutrino mass matrix M_ν . The two-zero patterns under discussion will serve as a good example to illustrate this strategy.

Our numerical results are presented in Figs. 1—14. Comments and discussions follow.

- **Pattern \mathbf{A}_1 .** Fig. 1 tells us that the neutrino mixing angles, in particular θ_{12} and θ_{23} , are actually insensitive to the Dirac CP-violating phase δ . This point can easily be understood with the help of Eq. (31) or Eq. (32), in which δ is only loosely related to the ratio of two neutrino mass-squared differences R_ν due to the smallness of θ_{13} . An interesting observation from the left panel of Fig. 1 is, that a relatively large value of θ_{13} (i.e., $\theta_{13} \approx 7^\circ \cdots 8^\circ$), which is quite close to the best-fit value $\theta_{13} = 8.3^\circ$ [16], is particularly favored. On the other hand, the neutrino mass spectrum is weakly hierarchical, as shown in Fig. 2. The dependence of m_1 and m_2 on δ is ascribed to the next-to-leading order corrections given in Eq. (30). We have also illustrated the numerical prediction for J_{CP} in Fig. 2. One can see the maximal value of J_{CP} is at the percent level and should be able to lead to observable effects of CP violation in a variety of long-baseline neutrino oscillation experiments. Because δ itself is essentially unconstrained by current experimental data at the 3σ level, ρ and σ turn out to be arbitrary as shown in Fig. 2, although their correlations with δ are rather sharp. Finally we remark that Pattern \mathbf{A}_1 of M_ν predicts $\langle m \rangle_{ee} = 0$ for the neutrinoless double-beta decay.
- **Pattern \mathbf{A}_2 .** As shown in Figs. 3 and 4, the phenomenological implications of Pattern \mathbf{A}_2 of M_ν are essentially the same as those of Pattern \mathbf{A}_1 . For instance, $\theta_{13} \approx 6^\circ \cdots 8^\circ$ is favored and the effective mass term $\langle m \rangle_{ee}$ is vanishing. Thus it is only necessary to emphasize their main difference. We have demonstrated a permutation symmetry between $M_\nu^{\mathbf{A}_1}$ and $M_\nu^{\mathbf{A}_2}$ in section 3.2 and found that the present best-fit values of neutrino mixing parameters (mainly $\theta_{23} = 40.4^\circ$ [16]) cannot coincide with Pattern \mathbf{A}_2 . If the maximal mixing angle $\theta_{23} = 45^\circ$ were finally established, however, it would be almost impossible to distinguish between Patterns \mathbf{A}_1 and \mathbf{A}_2 in practice.
- **Pattern \mathbf{B}_1 .** Since $m_2 > m_1$, we have $\cos \delta < 0$ (i.e., $\pi/2 < \delta < 3\pi/2$) in this case. In our numerical analysis we only focus on the range $\delta \in [\pi/2, \pi]$, because the range $\delta \in [\pi, 3\pi/2]$ can similarly be analyzed. As shown in Figs. 5 and 6, only a very narrow region $\delta \in [0.50\pi, 0.56\pi]$ is phenomenologically allowed. This result obviously originates from Eq. (42), where $|\cos \delta|$ must be small enough to suppress the magnitude of R_ν . Furthermore, we only consider the normal neutrino mass hierarchy corresponding to $\theta_{23} < 45^\circ$. The latter seems to be favored by current data at the 1σ level [16]. Fig. 5 shows that $\theta_{13} \sim 3^\circ$ and $\theta_{23} \sim 37^\circ$ are more likely. A strong correlation between θ_{23} and δ

can also be understood from Eq. (42); namely, the maximal mixing $\theta_{23} \approx 45^\circ$ requires the maximal CP-violating phase $\delta \approx \pi/2$. In addition, a nearly degenerate mass spectrum as shown in Fig. 6 is predicted. There is a lower bound on $\langle m \rangle_{ee}$ (i.e., $\langle m \rangle_{ee} \geq 0.03$ eV), which will be tested in the future experiments of the neutrinoless double-beta decay. Note that $\langle m \rangle_{ee} \approx 0.2$ eV can be achieved when $\theta_{23} \approx 45^\circ$ and $\delta \approx \pi/2$. The other three patterns of this category (i.e., **B₂**, **B₃** and **B₄**) have similar consequences, for which the numerical results have been given in Figs. 7 and 8, Figs. 9 and 10, and Figs. 11 and 12, respectively. But the details of these patterns, such as the allowed ranges of (ρ, σ, δ) and (m_1, m_2, m_3) , are somewhat different.

- **Pattern C.** Fig. 13 shows no significant preference in the allowed ranges of three neutrino mixing angles. A strong correlation between θ_{23} and δ only appears when δ is close to $\pi/2$. As shown in Fig. 14 and discussed in section 3.3, the inverted neutrino mass hierarchy is allowed in most parts of the parameter space (and a normal mass hierarchy is possible only when θ_{23} is very close to 45° and θ_{13} is nonvanishing). Like Patterns **B_{1,2,3,4}**, there is a lower bound on $\langle m \rangle_{ee}$ in Pattern **C** (i.e., $\langle m \rangle_{ee} > 0.02$ eV), and its maximal value can saturate the present experimental upper bound $\langle m \rangle_{ee} < 0.3$ eV [24]. It should be noted that the sum of the three neutrino masses is subject to the cosmological bound $\sum m_i < 0.58$ eV at the 95% confidence level [25], which has been derived from the seven-year WMAP data on the cosmic background radiation combined with the Baryon Acoustic Oscillations. Therefore, the possibility of $\delta \sim \pi/2$ is essentially excluded at the same confidence level. Similar conclusions apply to Patterns **B_{1,2,3,4}**.

Finally it is worth pointing out that we have also done a numerical analysis of the two-zero textures of M_ν by using the 1σ and 2σ values of δm^2 , Δm^2 , θ_{12} , θ_{23} and θ_{13} (see Table 1 and Ref. [16]). We find that all the seven patterns discussed above are compatible with current experimental data at the 1σ or 2σ level, although the corresponding parameter space is somewhat smaller. To be conservative, we take our numerical results obtained at the 3σ level more seriously.

5 Texture Zeros from Flavor Symmetries

In general, the texture zeros of a Majorana neutrino mass matrix can be realized in various seesaw models with proper discrete flavor symmetries. It is possible to obtain the zeros in arbitrary entries of a fermion mass matrix by means of the Abelian symmetries (e.g., the cyclic group Z_n [26]). To illustrate how to realize the two-zero textures of M_ν discussed above, we shall work in the type-II seesaw model, which extends the scalar sector of the standard model with one or more $SU(2)_L$ scalar triplets [20]. For N scalar triplets, the gauge-invariant Lagrangian relevant for neutrino masses reads

$$-\mathcal{L}_\Delta = \frac{1}{2} \sum_j \sum_{\alpha, \beta} (Y_{\Delta_j})_{\alpha\beta} \overline{\ell_{\alpha L}} \Delta_j i\sigma_2 \ell_{\beta L}^c + \text{h.c.}, \quad (66)$$

where α and β run over e, μ and τ , Δ_j denotes the j -th triplet scalar field (for $j = 1, 2, \dots, N$), and Y_{Δ_j} is the corresponding Yukawa coupling matrix. After the triplet scalar acquires its vacuum expectation value $\langle \Delta_j \rangle \equiv v_{\Delta_j}$, the Majorana neutrino mass matrix is given by

$$M_\nu = \sum_j Y_{\Delta_j} v_{\Delta_j}, \quad (67)$$

where the smallness of v_{Δ_j} is attributed to the largeness of the triplet scalar mass scale [20].

In order to generate the texture zeros in M_ν and derive the seven viable patterns $\mathbf{A}_{1,2}$, $\mathbf{B}_{1,2,3,4}$ and \mathbf{C} , we follow the spirit of Ref. [27] and impose the Z_n symmetry on the Lagrangian in Eq. (66). The unique generator of the cyclic group Z_n is $\varpi = e^{i2\pi/n}$, which produces all the group elements $Z_n = \{\mathbf{1}, \varpi, \varpi^2, \dots, \varpi^{n-1}\}$. Now it is straightforward to specify the number of scalar triplets N (i.e., $j = 1, 2, \dots, N$), the order of the cyclic group n and the representations of ℓ_α and Δ_j under the symmetry group.

- $N = 3$ and $n = 6$ for $\mathbf{A}_{1,2}$ and $\mathbf{B}_{3,4}$. In this case we have to introduce three scalar triplets and the Z_6 symmetry group, for which the generator is $\varpi = e^{i\pi/3}$. The representations of lepton doublets $\ell_{\alpha L}$ (for $\alpha = e, \mu, \tau$) and the scalar triplets Δ_j (for $j = 1, 2, 3$) are assigned as follows.

1. For Pattern \mathbf{A}_1 :

$$\begin{aligned} \ell_{eL} &\rightarrow \varpi^2 \ell_{eL}, & \ell_{\mu L} &\rightarrow \mathbf{1} \ell_{\mu L}, & \ell_{\tau L} &\rightarrow \varpi^3 \ell_{\tau L}, \\ \Delta_1 &\rightarrow \mathbf{1} \Delta_1, & \Delta_2 &\rightarrow \varpi^3 \Delta_2, & \Delta_3 &\rightarrow \varpi \Delta_3. \end{aligned} \quad (68)$$

Given the above representations of lepton doublets, three scalar triplets are needed to enforce the nonzero elements in the neutrino mass matrix: Δ_1 for $(M_\nu)_{\mu\mu}$ and $(M_\nu)_{\tau\tau}$, Δ_2 for $(M_\nu)_{\mu\tau}$ and Δ_3 for $(M_\nu)_{e\tau}$.

2. For Pattern \mathbf{A}_2 :

$$\begin{aligned} \ell_{eL} &\rightarrow \varpi^2 \ell_{eL}, & \ell_{\mu L} &\rightarrow \mathbf{1} \ell_{\mu L}, & \ell_{\tau L} &\rightarrow \varpi^3 \ell_{\tau L}, \\ \Delta_1 &\rightarrow \mathbf{1} \Delta_1, & \Delta_2 &\rightarrow \varpi^3 \Delta_2, & \Delta_3 &\rightarrow \varpi^4 \Delta_3. \end{aligned} \quad (69)$$

Note that Eq. (69) differs from Eq. (68) only in the assignment for the triplet Δ_3 . Such a difference originates from the fact that $(M_\nu)_{e\mu} = 0$ and $(M_\nu)_{e\tau} \neq 0$ hold for Pattern \mathbf{A}_1 , while $(M_\nu)_{e\tau} = 0$ and $(M_\nu)_{e\mu} \neq 0$ hold for Pattern \mathbf{A}_2 . It is worthwhile to point out that the assignments in Eq. (69) are by no means unique. As we have discussed in section 3.2, there exists a permutation symmetry between \mathbf{A}_1 and \mathbf{A}_2 . Therefore, we may exchange the representations of $\ell_{\mu L}$ and $\ell_{\tau L}$ in Eq. (68) but preserve those of scalar triplets to obtain \mathbf{A}_2 from \mathbf{A}_1 .

3. For Pattern \mathbf{B}_3 :

$$\begin{aligned} \ell_{eL} &\rightarrow \mathbf{1} \ell_{eL}, & \ell_{\mu L} &\rightarrow \varpi^2 \ell_{\mu L}, & \ell_{\tau L} &\rightarrow \varpi^3 \ell_{\tau L}, \\ \Delta_1 &\rightarrow \mathbf{1} \Delta_1, & \Delta_2 &\rightarrow \varpi^3 \Delta_2, & \Delta_3 &\rightarrow \varpi \Delta_3. \end{aligned} \quad (70)$$

4. For Pattern \mathbf{B}_4 :

$$\begin{aligned} \ell_{eL} &\rightarrow \varpi^3 \ell_{eL}, & \ell_{\mu L} &\rightarrow \mathbf{1} \ell_{\mu L}, & \ell_{\tau L} &\rightarrow \varpi^2 \ell_{\tau L}, \\ \Delta_1 &\rightarrow \mathbf{1} \Delta_1, & \Delta_2 &\rightarrow \varpi^3 \Delta_2, & \Delta_3 &\rightarrow \varpi^4 \Delta_3. \end{aligned} \quad (71)$$

In addition to the permutation symmetry P_{23} discussed in section 3.2, we notice that the location of texture zeros in Pattern \mathbf{B}_3 can be obtained from that in Pattern \mathbf{A}_1 by a permutation in the 1-2 rows and 1-2 columns. Similarly there exists a 1-3 permutation symmetry between Pattern \mathbf{B}_4 and Pattern \mathbf{A}_2 . Although these symmetries cannot lead to simple relations between any two of the neutrino mixing parameters, they are instructive for the assignments of lepton doublets. For instance, Eq. (70) and Eq. (71) can be derived from Eq. (68) and Eq. (69) by exchanging the representations of ℓ_{eL} and $\ell_{\mu L}$ and the representations of ℓ_{eL} and $\ell_{\tau L}$, respectively. The assignments of scalar triplets should not be changed.

- $N = 2$ and $n = 3$ for $\mathbf{B}_{1,2}$. In this case we introduce only two scalar triplets and the Z_3 symmetry group, for which the generator is $\varpi = e^{2i\pi/3}$. The assignments of lepton doublets $\ell_{\alpha L}$ (for $\alpha = e, \mu, \tau$) and the scalar triplets Δ_j (for $j = 1, 2$) are as follows.

1. For Pattern \mathbf{B}_1 :

$$\ell_{eL} \rightarrow \mathbf{1} \ell_{eL}, \quad \ell_{\mu L} \rightarrow \varpi \ell_{\mu L}, \quad \ell_{\tau L} \rightarrow \varpi^2 \ell_{\tau L}, \quad \Delta_1 \rightarrow \mathbf{1} \Delta_1, \quad \Delta_2 \rightarrow \varpi^2 \Delta_2. \quad (72)$$

2. For Pattern \mathbf{B}_2 :

$$\ell_{eL} \rightarrow \mathbf{1} \ell_{eL}, \quad \ell_{\mu L} \rightarrow \varpi^2 \ell_{\mu L}, \quad \ell_{\tau L} \rightarrow \varpi \ell_{\tau L}, \quad \Delta_1 \rightarrow \mathbf{1} \Delta_1, \quad \Delta_2 \rightarrow \varpi^2 \Delta_2. \quad (73)$$

Note that the assignment in Eq. (73) is slightly different from that in Ref. [27], where $\Delta_2 \rightarrow \varpi \Delta_2$ is taken and the representations of lepton doublets are the same as in Eq. (72). Here we have implemented the 2-3 permutation symmetry between Pattern \mathbf{B}_1 and Pattern \mathbf{B}_2 .

- $N = 3$ and $n = 4$ for Pattern \mathbf{C} . In this case we have to introduce three scalar triplets and the Z_4 symmetry group, for which the generator is $\varpi = e^{i\pi/2}$. The assignments of lepton doublets $\ell_{\alpha L}$ (for $\alpha = e, \mu, \tau$) and the scalar triplets Δ_j (for $j = 1, 2, 3$) are

$$\begin{aligned} \ell_{eL} &\rightarrow \mathbf{1} \ell_{eL}, & \ell_{\mu L} &\rightarrow \varpi \ell_{\mu L}, & \ell_{\tau L} &\rightarrow \varpi^3 \ell_{\tau L}, \\ \Delta_1 &\rightarrow \mathbf{1} \Delta_1, & \Delta_2 &\rightarrow \varpi^3 \Delta_2, & \Delta_3 &\rightarrow \varpi \Delta_3. \end{aligned} \quad (74)$$

Thus all the seven two-zero patterns of M_ν can be obtained in this simple symmetry scheme.

In all cases we have taken the right-handed charged-lepton singlets $E_{\alpha R}$ to transform in the same way as the left-handed lepton doublets $\ell_{\alpha L}$ and taken the standard-model Higgs doublet H to be in the trivial representation. Hence the charged-lepton mass matrix M_l is diagonal, as we have chosen from the beginning. The two-zero textures of M_ν can also be realized in the seesaw models with three right-handed neutrinos, several Higgs singlets, doublets and triplets, by imposing either Abelian or non-Abelian discrete flavor symmetries [26, 27, 28].

6 Summary

In view of the latest T2K and MINOS neutrino oscillation data which hint at a relatively large value of θ_{13} , we have performed a systematic study of the Majorana neutrino mass matrix M_ν with two independent texture zeros. It turns out that seven patterns (i.e., $\mathbf{A}_{1,2}$, $\mathbf{B}_{1,2,3,4}$ and \mathbf{C}) can survive current experimental tests at the 3σ level, although they are also compatible with the data at the 1σ or 2σ level. The following is a brief summary of our main observations:

- Given the values of three flavor mixing angles ($\theta_{12}, \theta_{23}, \theta_{13}$) and two neutrino mass-squared differences ($\delta m^2, \Delta m^2$), it is in principle possible to fully determine three CP-violating phases (δ, ρ, σ) and three neutrino masses (m_1, m_2, m_3). The analytical formulas for the latter have been derived and listed in Tables 2–4.
- By making the analytical approximations and taking the best-fit values of neutrino mixing parameters [16], we find that only Pattern \mathbf{A}_2 can be excluded. We have numerically confirmed that all the seven patterns of M_ν (i.e., $\mathbf{A}_{1,2}$, $\mathbf{B}_{1,2,3,4}$ and \mathbf{C}) are compatible with current neutrino oscillation data at the 1σ level, but our numerical results have been presented only at the more conservative 3σ level.
- Figs. 1–14 show the main numerical results of our systematic analysis. Some interesting points should be emphasized. (1) Both \mathbf{A}_1 and \mathbf{A}_2 favor a relatively large θ_{13} (e.g., $\theta_{13} \sim 8^\circ$), $\mathbf{B}_{1,2,3,4}$ prefer a relatively small θ_{13} (e.g., $\theta_{13} \sim 3^\circ$), and \mathbf{C} shows no significant preference for the magnitude of θ_{13} . (2) The Dirac CP-violating phase δ obtained from $\mathbf{B}_{1,2,3,4}$ lies in a narrow range around $\pi/2$ or $3\pi/2$, and $\delta = \pi/2$ is strongly correlated with $\theta_{23} = \pi/4$. (3) For $\delta \rightarrow \pi/2$ and $\theta_{23} \rightarrow \pi/4$, the predictions for neutrino masses m_i and the effective neutrino mass $\langle m \rangle_{ee}$ may run into contradiction with their upper bounds set by the cosmological observations and the neutrinoless double-beta decay experiments. (4) The size of J_{CP} may reach the percent level and thus appreciable leptonic CP violation is possible to show up in the future long-baseline neutrino oscillation experiments.

In addition we have shown that the texture zeros of the Majorana neutrino mass matrix M_ν are stable against the one-loop quantum corrections⁶, and pointed out that there exists a permutation symmetry between \mathbf{A}_1 and \mathbf{A}_2 , \mathbf{B}_1 and \mathbf{B}_2 or \mathbf{B}_3 and \mathbf{B}_4 . In the type-II seesaw model with two or three scalar triplets we have illustrated how to realize two-zero textures of M_ν by using the Z_n flavor symmetry.

The ongoing and upcoming neutrino oscillation experiments are expected to measure the neutrino mixing parameters, in particular the smallest mixing angle θ_{13} , the deviation of θ_{23} from $\pi/4$ and the Dirac CP-violating phase δ . The sensitivity of future cosmological observations to the sum of neutrino masses $\sum m_i$ and the sensitivity of the neutrinoless double-beta decay experiments to the effective mass term $\langle m \rangle_{ee}$ will probably reach ~ 0.05 eV in the near

⁶In contrast, the texture zeros of the Dirac neutrino mass matrix are essentially sensitive to quantum corrections like those of quark mass matrices [29].

future. We therefore expect that some patterns of the two-zero textures of M_ν might be excluded or only marginally allowed by tomorrow's data, and those capable of surviving should shed light on the underlying flavor structures of massive neutrinos.

Acknowledgements

This work was supported in part by the National Natural Science Foundation of China under grant No. 10875131 (Z.Z.X.) and by the Alexander von Humboldt Foundation (S.Z.).

References

- [1] Particle Data Group, K. Nakamura *et al.*, J. Phys. G **37**, 075021 (2010).
- [2] T2K Collaboration, K. Abe *et al.*, Phys. Rev. Lett. **107**, 041801 (2011).
- [3] MINOS Collaboration, P. Adamson *et al.*, arXiv:1108.0015.
- [4] Double Chooz Collaboration, F. Ardellier *et al.*, hep-ex/0606025.
- [5] Daya Bay Collaboration, X. Guo *et al.*, hep-ex/0701029.
- [6] RENO Collaboration, J.K. Ahn *et al.*, arXiv:1003.1391.
- [7] H. Fritzsch and Z.Z. Xing, Prog. Part. Nucl. Phys. **45**, 1 (2000); Z.Z. Xing, Int. J. Mod. Phys. A **19**, 1 (2004).
- [8] C.D. Froggatt and H.B. Nielsen, Nucl. Phys. B **147**, 277 (1979).
- [9] Z.Z. Xing, hep-ph/0406049.
- [10] P.H. Frampton, S.L. Glashow, and D. Marfatia, Phys. Lett. B **536**, 79 (2002).
- [11] Z.Z. Xing, Phys. Lett. B **530**, 159 (2002).
- [12] Z.Z. Xing, Phys. Lett. B **539**, 85 (2002).
- [13] W.L. Guo and Z.Z. Xing, Phys. Rev. D **67**, 053002 (2003).
- [14] See, e.g., P.H. Frampton, M.C. Oh, and T. Yoshikawa, Phys. Rev. D **66**, 033007 (2002); A. Kageyama, S. Kaneko, N. Shimoyama, and M. Tanimoto, Phys. Lett. B **538**, 96 (2002); B.R. Desai, D.P. Roy, and A.R. Vaucher, Mod. Phys. Lett. A **18**, 1355 (2003); M. Frigerio and A.Yu. Smirnov, Phys. Rev. D **67**, 013007 (2003); M. Honda, S. Kaneko, and M. Tanimoto, JHEP **0309**, 028 (2003); G. Bhattacharyya, A. Raychaudhuri, and A. Sil, Phys. Rev. D **67**, 073004 (2003); A. Watanabe and K. Yoshioka, JHEP **0605**, 044 (2006); R. Mohanta, G. Kranti, and A.K. Giri, hep-ph/0608292; Y. Farzan and A.Yu. Smirnov, JHEP **0701**, 059 (2007); S. Dev, S. Kumar, S. Verma, and S. Gupta, Nucl. Phys. B **784**, 103 (2007); Phys. Rev. D **76**, 013002 (2007); W.L. Guo, Z.Z. Xing, and S. Zhou, Int. Mod. Phys. E **16**, 1 (2007); S. Rajpoot, hep-ph/0703185; H.A. Alhendi, E.I. Lashin, A.A. Mudlei, Phys. Rev. D **77**, 013009 (2008); E.I. Lashin and N. Chamoun, Phys. Rev. D **78**, 073002 (2008); A. Dighe and N. Sahu, arXiv:0812.0695; S. Goswami and A. Watanabe, Phys. Rev. D **79**, 033004 (2009); S. Choubey, W. Rodejohann, and P. Roy, Nucl. Phys. B **808**, 272 (2009); S. Dev, S. Kumar, and S. Verma, Phys. Rev. D **79**, 033011 (2009); G. Ahuja, M. Gupta, M. Randhawa, and R. Verma, Phys. Rev. D **79**, 093006 (2009); S. Goswami, S. Khan, and W. Rodejohann, Phys. Lett. B **680**, 255 (2009); E.I. Lashin and N. Chamoun, Phys. Rev. D **80**, 093004 (2009); S. Dev, S. Verma, and S. Gupta, Phys.

- Lett. B **687**, 53 (2010); S. Dev, S. Gupta, and R.R. Gautam, Phys. Rev. D **82**, 073015 (2010); W. Grimus and P.O. Ludl, Phys. Lett. B **700**, 356 (2011).
- [15] See, e.g., Z.Z. Xing, Phys. Rev. D **68**, 053002 (2003); Phys. Rev. D **69**, 013006 (2004); A. Merle and W. Rodejohann, Phys. Rev. D **73**, 073012 (2006); Y. BenTov and A. Zee, arXiv:1103.2616; E.I. Lashin and N. Chamoun, arXiv:1108.4010.
- [16] G.L. Fogli *et al.*, arXiv:1106.6028.
- [17] T. Schwetz, M. Tortola, and J.W.F. Valle, arXiv:1108.1376.
- [18] S. Weinberg, Phys. Rev. Lett. **43**, 1566 (1978).
- [19] P. Minkowski, Phys. Lett. B **67**, 421 (1977); T. Yanagida, in *Proceedings of the Workshop on Unified Theory and the Baryon Number of the Universe*, edited by O. Sawada and A. Sugamoto (KEK, Tsukuba, 1979); M. Gell-Mann, P. Ramond, and R. Slansky, in *Supergravity*, edited by P. van Nieuwenhuizen and D. Freedman (North Holland, Amsterdam, 1979); S.L. Glashow, in *Quarks and Leptons*, edited by M. Lévy *et al.* (Plenum, New York, 1980); R.N. Mohapatra and G. Senjanovic, Phys. Rev. Lett. **44**, 912 (1980).
- [20] W. Konetschny and W. Kummer, Phys. Lett. B **70**, 433 (1977); J. Schechter and J.W.F. Valle, Phys. Rev. D **22**, 2227 (1980); T.P. Cheng and L.F. Li, Phys. Rev. D **22**, 2860 (1980); M. Magg and C. Wetterich, Phys. Lett. B **94**, 61 (1980); G. Lazarides, Q. Shafi, and C. Wetterich, Nucl. Phys. B **181**, 287 (1981); R.N. Mohapatra and G. Senjanovic, Phys. Rev. D **23**, 165 (1981).
- [21] R. Foot, H. Lew, X.G. He, and G.C. Joshi, Z. Phys. C **44**, 441 (1989).
- [22] See, e.g., P.H. Chankowski and Z. Pluciennik, Phys. Lett. B **316**, 312 (1993); K.S. Babu, C.N. Leung, and J. Pantaleone, Phys. Lett. B **319**, 191 (1993).
- [23] J.W. Mei and Z.Z. Xing, Phys. Rev. D **69**, 073003 (2004).
- [24] G.L. Fogli *et al.*, Phys. Rev. D **78**, 033010 (2008); S.M. Bilenky, Phys. Part. Nucl. **41**, 690 (2010); W. Rodejohann, arXiv:1106.1334.
- [25] E. Komatsu *et al.*, Astrophys. J. Suppl. **192**, 18 (2011).
- [26] W. Grimus, A.S. Joshipura, L. Lavoura, and M. Tanimoto, Eur. Phys. J. C **36**, 227 (2004).
- [27] W. Grimus and L. Lavoura, J. Phys. G **31**, 693 (2005); Z.Z. Xing and S. Zhou, Phys. Lett. B **679**, 249 (2009).
- [28] See, e.g., M. Frigerio, S. Kaneko, E. Ma, M. Tanimoto, Phys. Rev. D **71**, 011901 (2005); M. Hirsch, A.S. Joshipura, S. Kaneko and J.W.F. Valle, Phys. Rev. Lett. **99**, 151802 (2007); S. Dev, S. Gupta, and R.R. Gautam, Phys. Lett. B **701**, 605 (2011).
- [29] C. Hagedorn and W. Rodejohann, JHEP **0507**, 034 (2005).

Table 2: Seven viable patterns of the neutrino mass matrix M_ν with two texture zeros, and their predictions for three CP-violating phases (δ, ρ, σ).

Pattern	Texture of M_ν	CP-violating phases
\mathbf{A}_1	$\begin{pmatrix} 0 & 0 & \times \\ 0 & \times & \times \\ \times & \times & \times \end{pmatrix}$	$\delta \approx \cos^{-1} \left[+ \frac{\tan \theta_{23}}{\tan 2\theta_{12} \sin \theta_{13}} \left(\frac{\sin 2\theta_{12} \tan 2\theta_{12} R_\nu}{4 \tan^2 \theta_{23} \sin^2 \theta_{13}} - 1 \right) \right]$ $\rho \approx \frac{\delta}{2}, \quad \sigma \approx \frac{\delta}{2} - \frac{\pi}{2}$
\mathbf{A}_2	$\begin{pmatrix} 0 & \times & 0 \\ \times & \times & \times \\ 0 & \times & \times \end{pmatrix}$	$\delta \approx \cos^{-1} \left[- \frac{\cot \theta_{23}}{\tan 2\theta_{12} \sin \theta_{13}} \left(\frac{\sin 2\theta_{12} \tan 2\theta_{12} R_\nu}{4 \cot^2 \theta_{23} \sin^2 \theta_{13}} - 1 \right) \right]$ $\rho \approx \frac{\delta}{2} - \frac{\pi}{2}, \quad \sigma \approx \frac{\delta}{2}$
\mathbf{B}_1	$\begin{pmatrix} \times & \times & 0 \\ \times & 0 & \times \\ 0 & \times & \times \end{pmatrix}$	$\delta \approx \cos^{-1} \left[- \frac{\sin 2\theta_{12} R_\nu}{2 \sin \theta_{13} \tan 2\theta_{23} } \right]$ $\rho \approx \sigma \approx \delta - \frac{\pi}{2}, \quad \rho - \sigma \approx - \frac{2 \sin \theta_{13} \sin \delta}{\sin 2\theta_{12} \tan 2\theta_{23} \tan^2 \theta_{23}}$
\mathbf{B}_2	$\begin{pmatrix} \times & 0 & \times \\ 0 & \times & \times \\ \times & \times & 0 \end{pmatrix}$	$\delta \approx \cos^{-1} \left[+ \frac{\sin 2\theta_{12} R_\nu}{2 \sin \theta_{13} \tan 2\theta_{23} } \right]$ $\rho \approx \sigma \approx \delta - \frac{\pi}{2}, \quad \rho - \sigma \approx - \frac{2 \sin \theta_{13} \sin \delta}{\sin 2\theta_{12} \tan 2\theta_{23} \cot^2 \theta_{23}}$
\mathbf{B}_3	$\begin{pmatrix} \times & 0 & \times \\ 0 & 0 & \times \\ \times & \times & \times \end{pmatrix}$	$\delta \approx \cos^{-1} \left[+ \frac{\sin 2\theta_{12} \cot^2 \theta_{23} R_\nu}{2 \sin \theta_{13} \tan 2\theta_{23} } \right]$ $\rho \approx \sigma \approx \delta - \frac{\pi}{2}, \quad \rho - \sigma \approx + \frac{2 \sin \theta_{13} \sin \delta}{\sin 2\theta_{12} \tan 2\theta_{23}}$
\mathbf{B}_4	$\begin{pmatrix} \times & \times & 0 \\ \times & \times & \times \\ 0 & \times & 0 \end{pmatrix}$	$\delta \approx \cos^{-1} \left[- \frac{\sin 2\theta_{12} \tan^2 \theta_{23} R_\nu}{2 \sin \theta_{13} \tan 2\theta_{23} } \right]$ $\rho \approx \sigma \approx \delta - \frac{\pi}{2}, \quad \rho - \sigma \approx + \frac{2 \sin \theta_{13} \sin \delta}{\sin 2\theta_{12} \tan 2\theta_{23}}$
\mathbf{C}	$\begin{pmatrix} \times & \times & \times \\ \times & 0 & \times \\ \times & \times & 0 \end{pmatrix}$	$\delta \approx \frac{2(1 + \tan \theta_{12} \tan \theta_{23}) + \tan^2 \theta_{12} \tan 2\theta_{12} \tan \theta_{23} R_\nu}{[1 + (1 - R_\nu) \tan \theta_{12} \tan \theta_{23}] \tan 2\theta_{12} \tan 2\theta_{23} \sin \theta_{13}}$ $\rho \approx \delta + \frac{1}{2} \tan^{-1} \left[\frac{\cot \theta_{12} \sin \delta}{\tan 2\theta_{23} \sin \theta_{13} - \cot \theta_{12} \cos \delta} \right] - \frac{\pi}{2}$ $\sigma \approx \delta - \frac{1}{2} \tan^{-1} \left[\frac{\tan \theta_{12} \sin \delta}{\tan 2\theta_{23} \sin \theta_{13} + \tan \theta_{12} \cos \delta} \right] - \frac{\pi}{2}$

Table 3: Seven viable patterns of the neutrino mass matrix M_ν with two texture zeros, and their predictions for two neutrino mass ratios $\xi \equiv m_1/m_3$ and $\zeta \equiv m_2/m_3$.

Pattern	Texture of M_ν	Neutrino mass ratios
\mathbf{A}_1	$\begin{pmatrix} 0 & 0 & \times \\ 0 & \times & \times \\ \times & \times & \times \end{pmatrix}$	$\xi \approx \tan \theta_{12} \tan \theta_{23} \sin \theta_{13}$, $\zeta \approx \cot \theta_{12} \tan \theta_{23} \sin \theta_{13}$
\mathbf{A}_2	$\begin{pmatrix} 0 & \times & 0 \\ \times & \times & \times \\ 0 & \times & \times \end{pmatrix}$	$\xi \approx \tan \theta_{12} \cot \theta_{23} \sin \theta_{13}$, $\zeta \approx \cot \theta_{12} \cot \theta_{23} \sin \theta_{13}$
\mathbf{B}_1	$\begin{pmatrix} \times & \times & 0 \\ \times & 0 & \times \\ 0 & \times & \times \end{pmatrix}$	$\xi \approx \zeta \approx \tan^2 \theta_{23}$, $\xi - \zeta \approx +\frac{4 \sin \theta_{13} \cos \delta}{\sin 2\theta_{12} \sin 2\theta_{23}}$
\mathbf{B}_2	$\begin{pmatrix} \times & 0 & \times \\ 0 & \times & \times \\ \times & \times & 0 \end{pmatrix}$	$\xi \approx \zeta \approx \cot^2 \theta_{23}$, $\xi - \zeta \approx -\frac{4 \sin \theta_{13} \cos \delta}{\sin 2\theta_{12} \sin 2\theta_{23}}$
\mathbf{B}_3	$\begin{pmatrix} \times & 0 & \times \\ 0 & 0 & \times \\ \times & \times & \times \end{pmatrix}$	$\xi \approx \zeta \approx \tan^2 \theta_{23}$, $\xi - \zeta \approx -\frac{4 \tan^2 \theta_{23} \sin \theta_{13} \cos \delta}{\sin 2\theta_{12} \sin 2\theta_{23}}$
\mathbf{B}_4	$\begin{pmatrix} \times & \times & 0 \\ \times & \times & \times \\ 0 & \times & 0 \end{pmatrix}$	$\xi \approx \zeta \approx \cot^2 \theta_{23}$, $\xi - \zeta \approx +\frac{4 \cot^2 \theta_{23} \sin \theta_{13} \cos \delta}{\sin 2\theta_{12} \sin 2\theta_{23}}$
\mathbf{C}	$\begin{pmatrix} \times & \times & \times \\ \times & 0 & \times \\ \times & \times & 0 \end{pmatrix}$	$\xi \approx \left(1 - \frac{2 \cot \theta_{12} \cos \delta}{\tan 2\theta_{23} \sin \theta_{13}} + \frac{\cot^2 \theta_{12}}{\tan^2 2\theta_{23} \sin^2 \theta_{13}}\right)^{1/2}$ $\zeta \approx \left(1 + \frac{2 \tan \theta_{12} \cos \delta}{\tan 2\theta_{23} \sin \theta_{13}} + \frac{\tan^2 \theta_{12}}{\tan^2 2\theta_{23} \sin^2 \theta_{13}}\right)^{1/2}$

Table 4: Seven viable patterns of the neutrino mass matrix M_ν with two texture zeros, and their predictions for the absolute neutrino mass m_3 and the effective mass terms of the neutrinoless double-beta decay $\langle m \rangle_{ee}$.

Pattern	Texture of M_ν	The scales of neutrino masses
\mathbf{A}_1	$\begin{pmatrix} 0 & 0 & \times \\ 0 & \times & \times \\ \times & \times & \times \end{pmatrix}$	$m_3 \approx \sqrt{\Delta m^2}, \quad \langle m \rangle_{ee} = 0$
\mathbf{A}_2	$\begin{pmatrix} 0 & \times & 0 \\ \times & \times & \times \\ 0 & \times & \times \end{pmatrix}$	$m_3 \approx \sqrt{\Delta m^2}, \quad \langle m \rangle_{ee} = 0$
\mathbf{B}_1	$\begin{pmatrix} \times & \times & 0 \\ \times & 0 & \times \\ 0 & \times & \times \end{pmatrix}$	$m_3 \approx \sqrt{\frac{\Delta m^2}{1 - \tan^4 \theta_{23}}}, \quad \langle m \rangle_{ee} \approx m_3 \tan^2 \theta_{23}$
\mathbf{B}_2	$\begin{pmatrix} \times & 0 & \times \\ 0 & \times & \times \\ \times & \times & 0 \end{pmatrix}$	$m_3 \approx \sqrt{\frac{\Delta m^2}{1 - \cot^4 \theta_{23}}}, \quad \langle m \rangle_{ee} \approx m_3 \cot^2 \theta_{23}$
\mathbf{B}_3	$\begin{pmatrix} \times & 0 & \times \\ 0 & 0 & \times \\ \times & \times & \times \end{pmatrix}$	$m_3 \approx \sqrt{\frac{\Delta m^2}{1 - \tan^4 \theta_{23}}}, \quad \langle m \rangle_{ee} \approx m_3 \tan^2 \theta_{23}$
\mathbf{B}_4	$\begin{pmatrix} \times & \times & 0 \\ \times & \times & \times \\ 0 & \times & 0 \end{pmatrix}$	$m_3 \approx \sqrt{\frac{\Delta m^2}{1 - \cot^4 \theta_{23}}}, \quad \langle m \rangle_{ee} \approx m_3 \cot^2 \theta_{23}$
\mathbf{C}	$\begin{pmatrix} \times & \times & \times \\ \times & 0 & \times \\ \times & \times & 0 \end{pmatrix}$	$m_3 \approx \sqrt{\frac{\tan^2 2\theta_{23} \cot^2 \theta_{12} \sin^2 \theta_{13} \Delta m^2}{1 + 2 \cot \theta_{12} \tan 2\theta_{23} \sin \theta_{13} \cos \delta}}$ $\langle m \rangle_{ee} \approx m_3 \sqrt{1 - \frac{4 \cot 2\theta_{12} \cos \delta}{\tan 2\theta_{23} \sin \theta_{13}} + \frac{4 \cot^2 2\theta_{12}}{\tan^2 2\theta_{23} \sin^2 \theta_{13}}}$

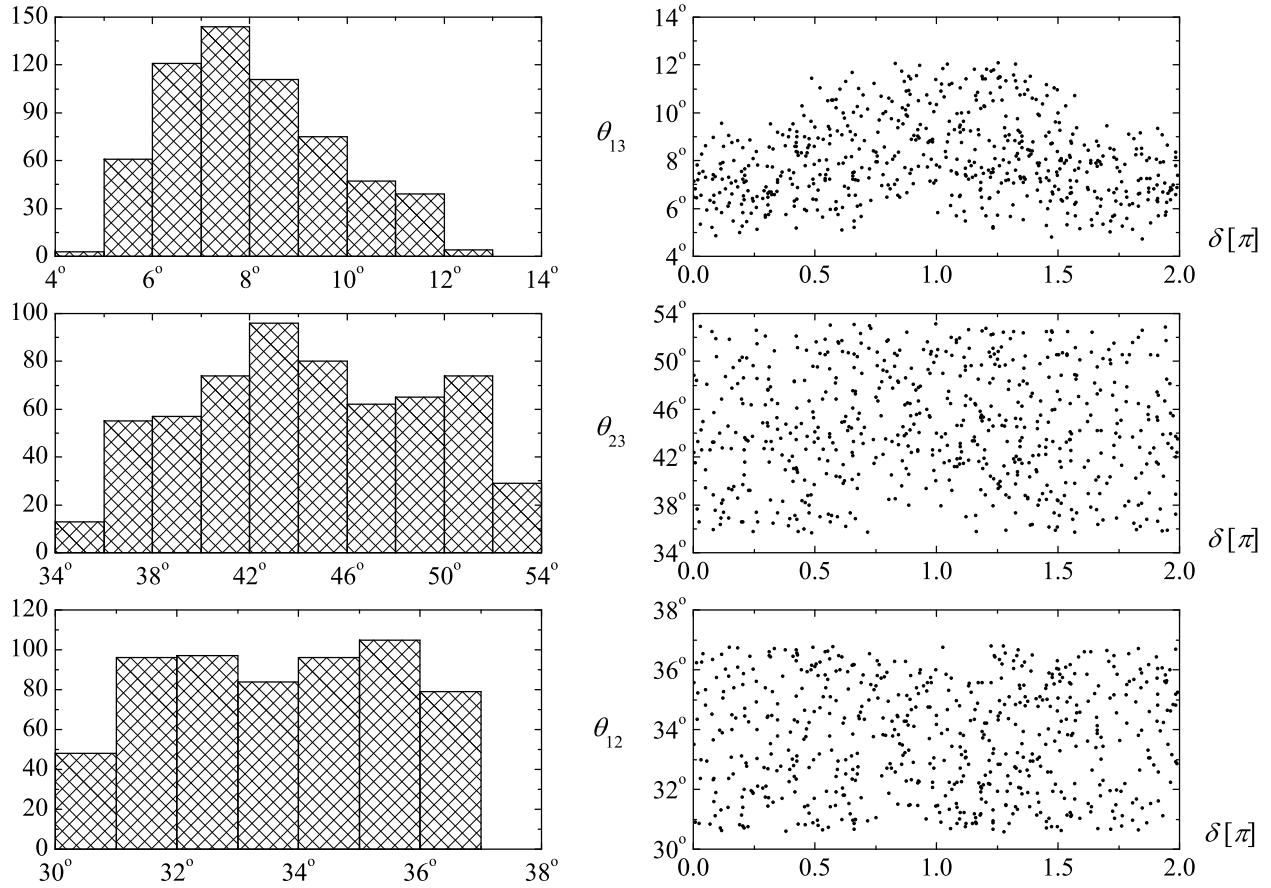


Figure 1: Pattern \mathbf{A}_1 of M_ν : allowed ranges of flavor mixing angles ($\theta_{12}, \theta_{23}, \theta_{13}$) versus the Dirac CP-violating phase δ at the 3σ level, where the probability distribution of three angles are shown in the left panel.

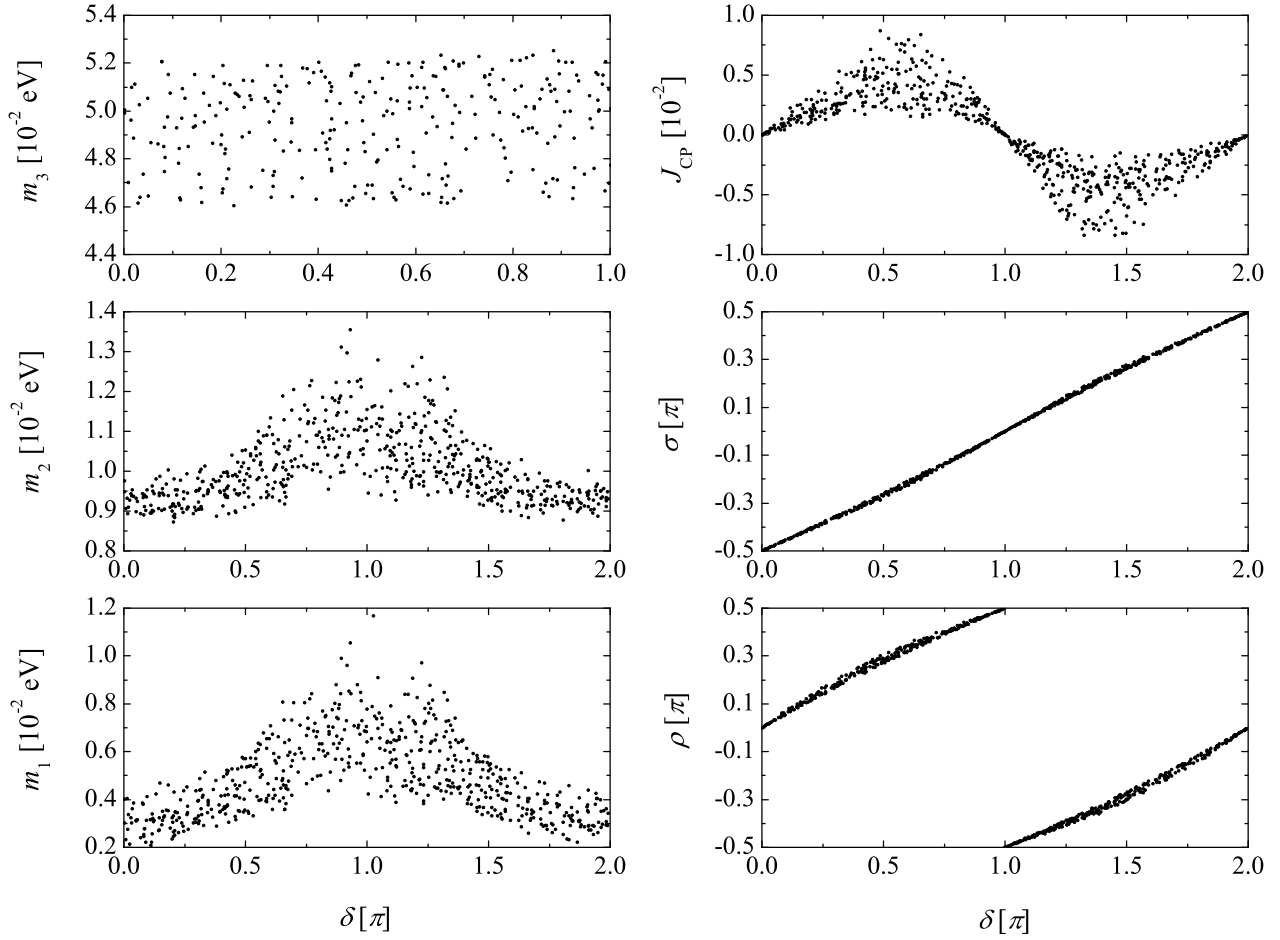


Figure 2: Pattern \mathbf{A}_1 of M_ν : allowed ranges of the neutrino masses (m_1, m_2, m_3), the Jarlskog invariant J_{CP} and the Majorana CP-violating phases (ρ, σ) versus the Dirac CP-violating phase δ at the 3σ level.

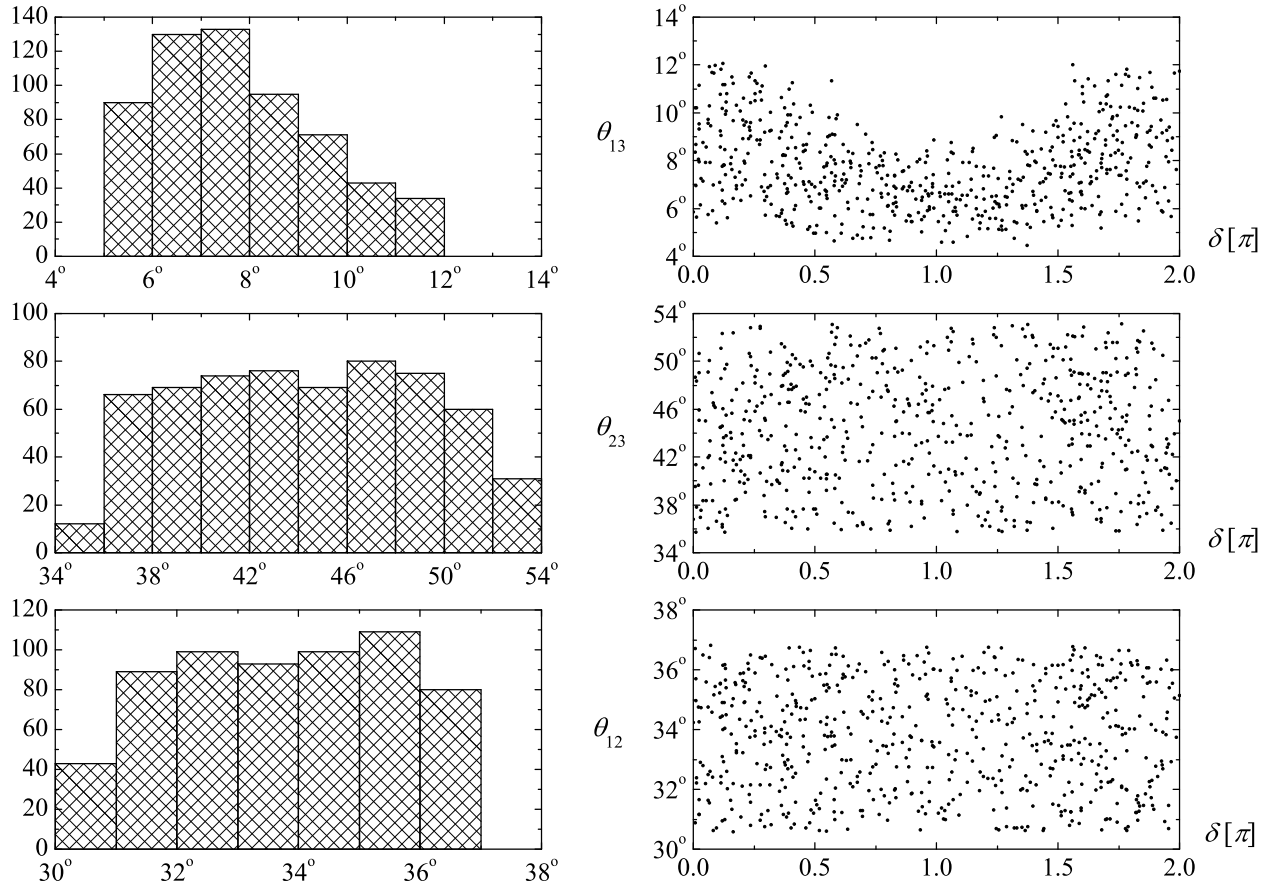


Figure 3: Pattern \mathbf{A}_2 of M_ν : allowed ranges of flavor mixing angles $(\theta_{12}, \theta_{23}, \theta_{13})$ versus the Dirac CP-violating phase δ at the 3σ level, where the probability distribution of three angles are shown in the left panel.

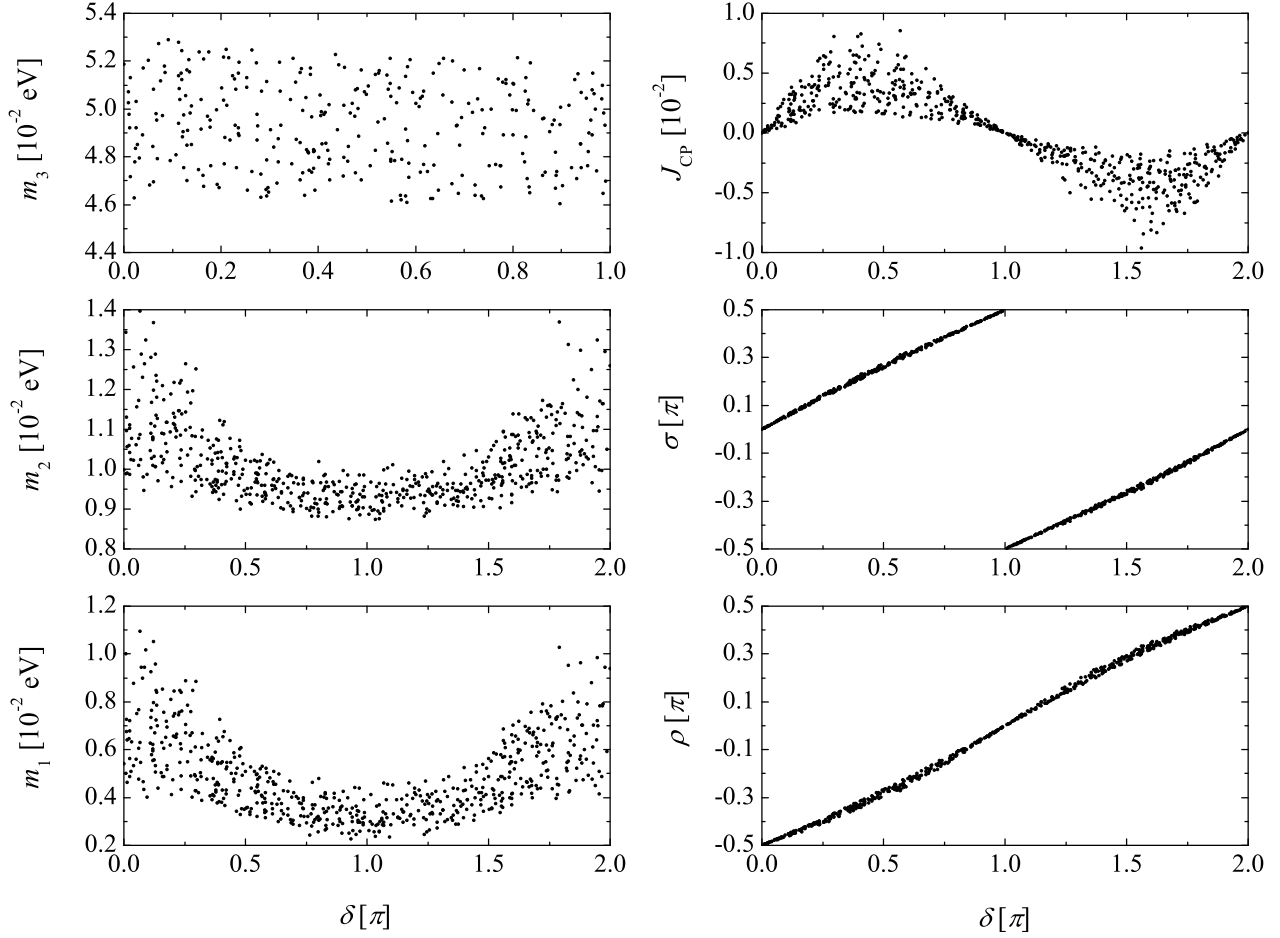


Figure 4: Pattern \mathbf{A}_2 of M_ν : allowed ranges of the neutrino masses (m_1, m_2, m_3), the Jarlskog invariant J_{CP} and the Majorana CP-violating phases (ρ, σ) versus the Dirac CP-violating phase δ at the 3σ level.

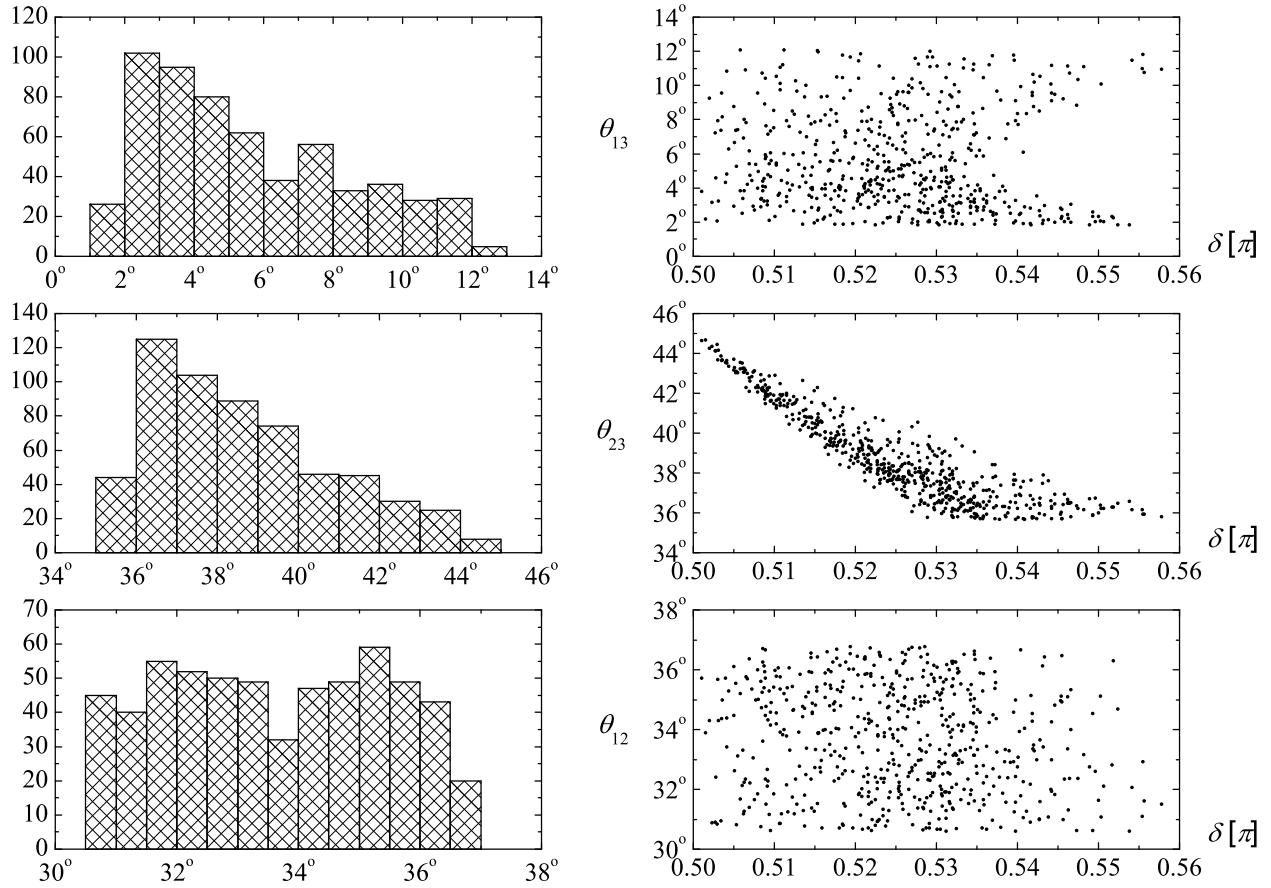


Figure 5: Pattern \mathbf{B}_1 of M_ν : allowed ranges of flavor mixing angles $(\theta_{12}, \theta_{23}, \theta_{13})$ versus the Dirac CP-violating phase δ at the 3σ level, where the probability distribution of three angles are shown in the left panel.

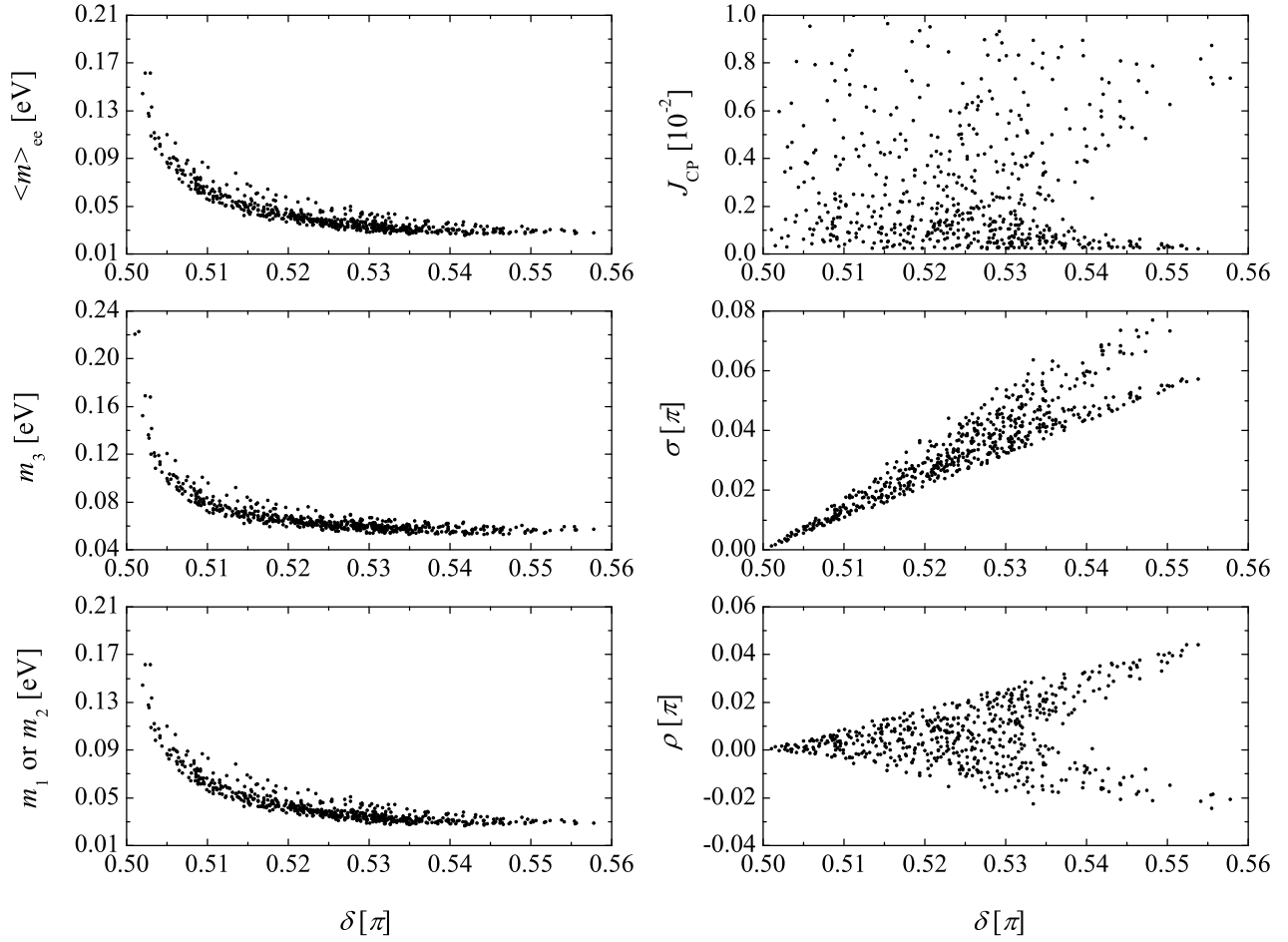


Figure 6: Pattern \mathbf{B}_1 of M_ν : allowed ranges of the neutrino masses (m_1, m_2, m_3), the Jarlskog invariant J_{CP} and the Majorana CP-violating phases (ρ, σ) versus the Dirac CP-violating phase δ at the 3σ level.

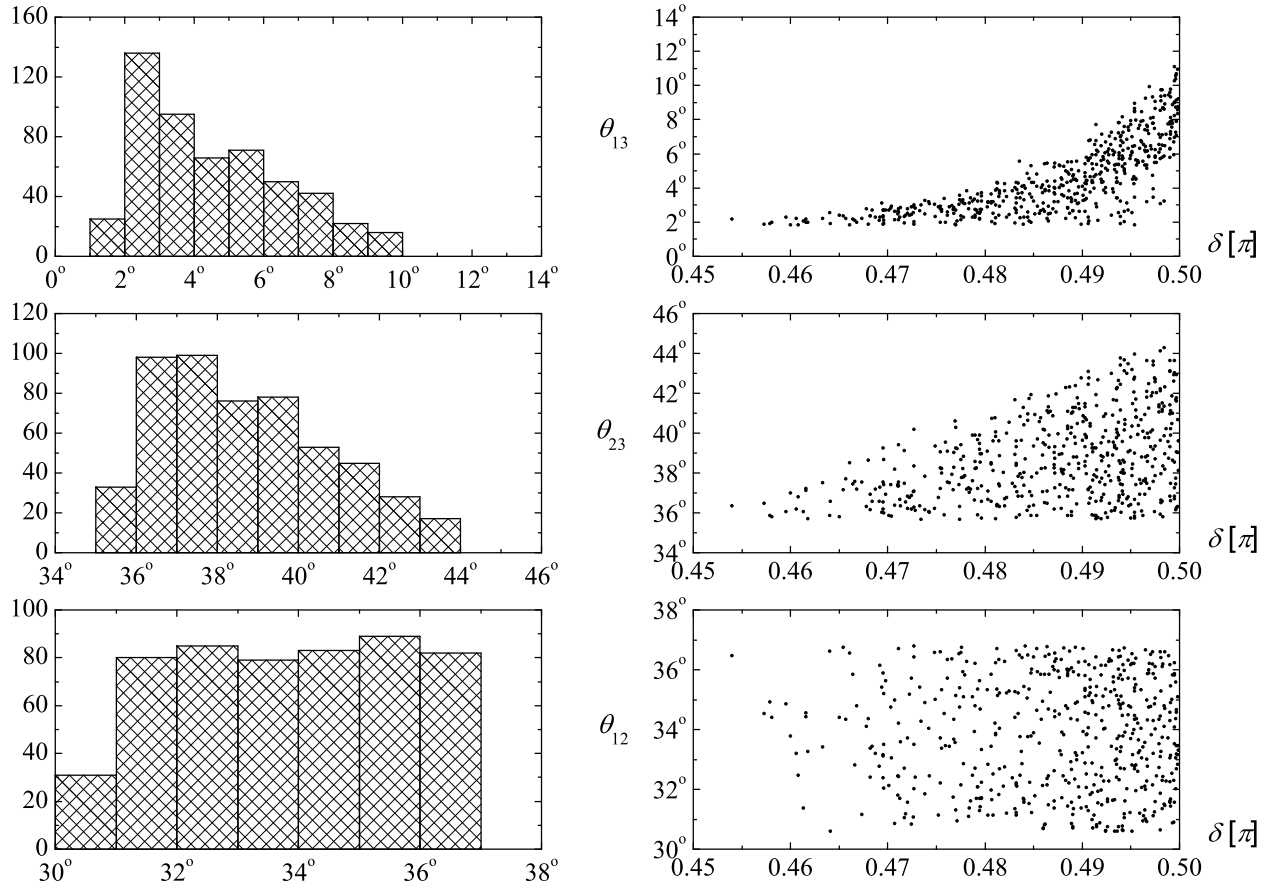


Figure 7: Pattern \mathbf{B}_2 of M_ν : allowed ranges of flavor mixing angles $(\theta_{12}, \theta_{23}, \theta_{13})$ versus the Dirac CP-violating phase δ at the 3σ level, where the probability distribution of three angles are shown in the left panel.

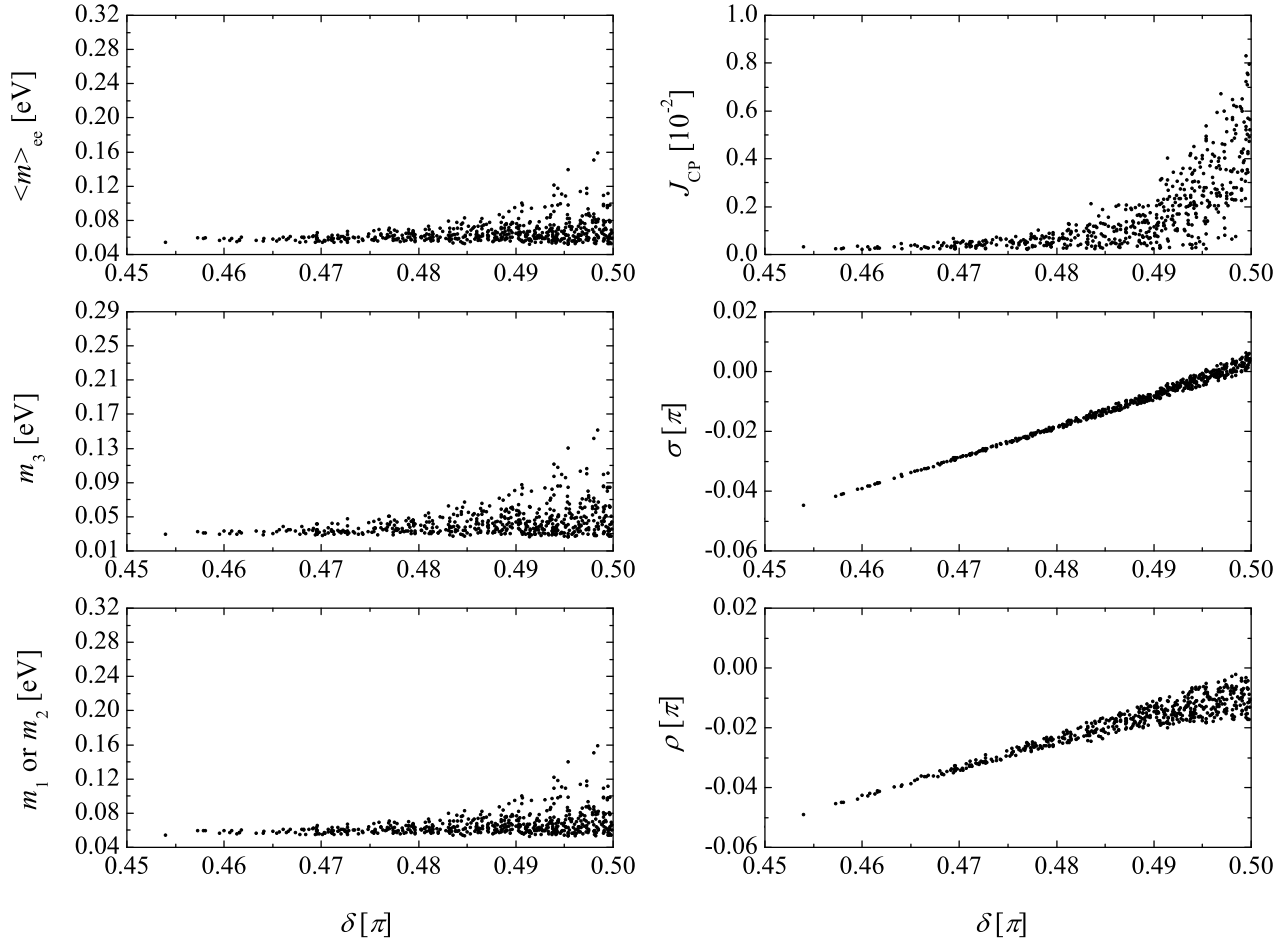


Figure 8: Pattern \mathbf{B}_2 of M_ν : allowed ranges of the neutrino masses (m_1, m_2, m_3), the Jarlskog invariant J_{CP} and the Majorana CP-violating phases (ρ, σ) versus the Dirac CP-violating phase δ at the 3σ level.

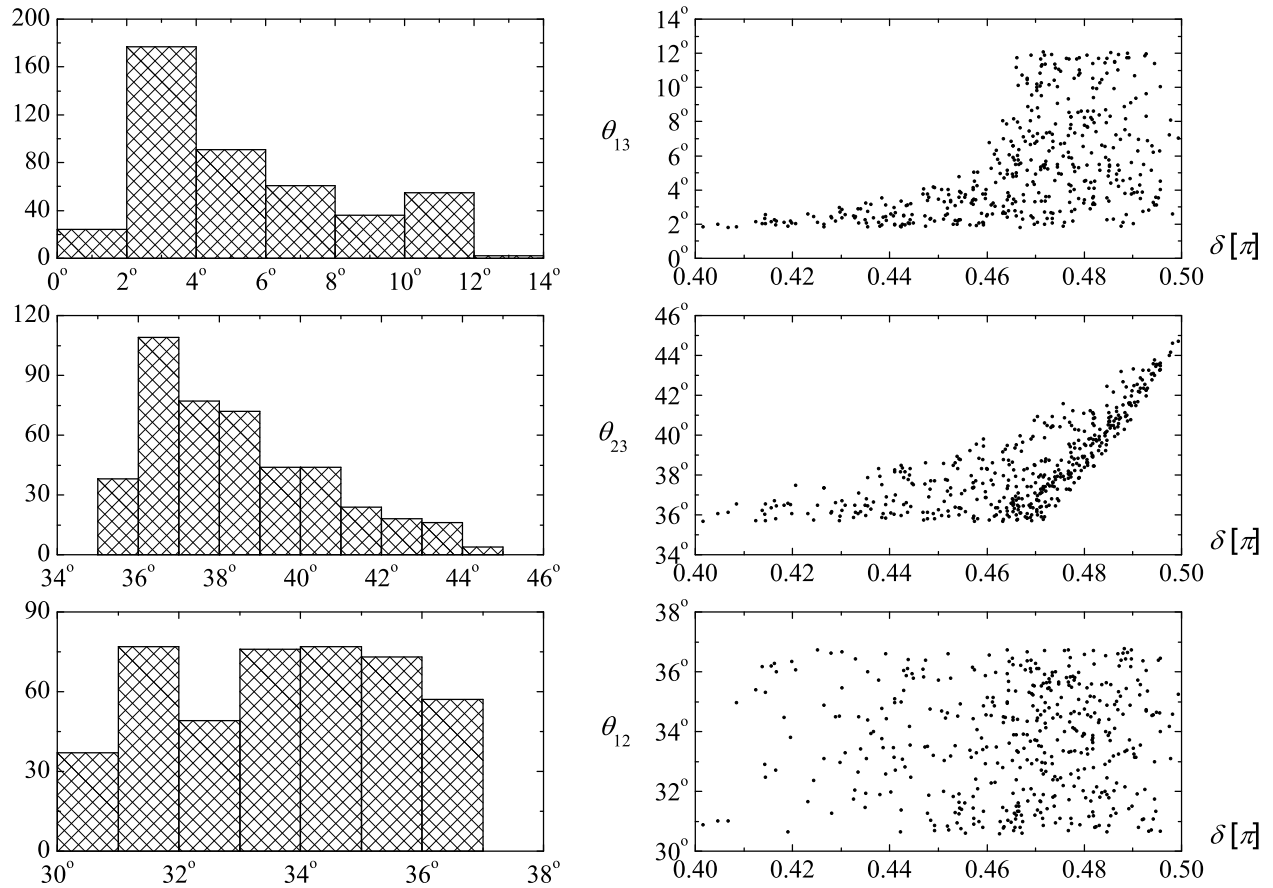


Figure 9: Pattern \mathbf{B}_3 of M_ν : allowed ranges of flavor mixing angles $(\theta_{12}, \theta_{23}, \theta_{13})$ versus the Dirac CP-violating phase δ at the 3σ level, where the probability distribution of three angles are shown in the left panel.

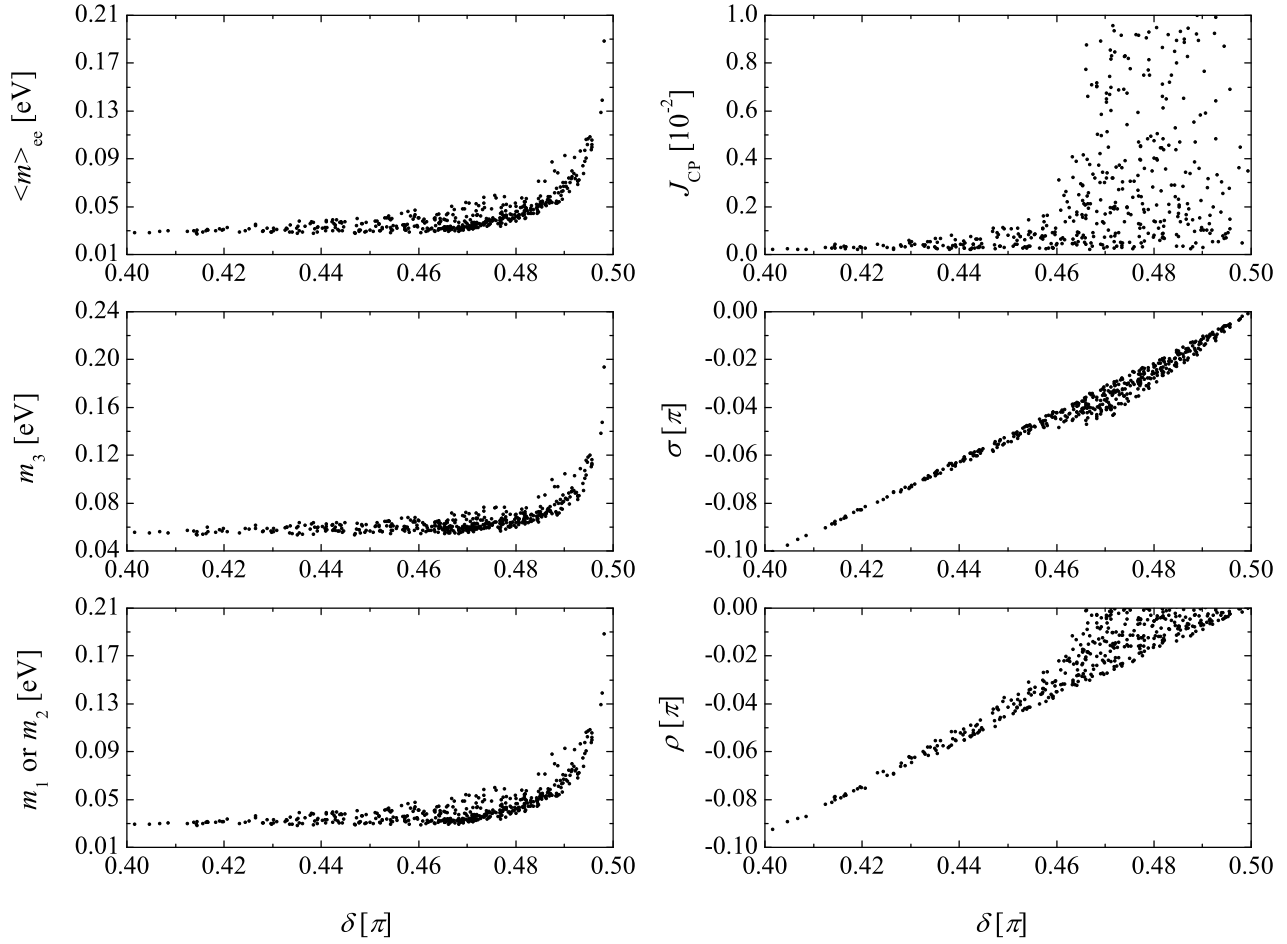


Figure 10: Pattern \mathbf{B}_3 of M_ν : allowed ranges of the neutrino masses (m_1, m_2, m_3), the Jarlskog invariant J_{CP} and the Majorana CP-violating phases (ρ, σ) versus the Dirac CP-violating phase δ at the 3σ level.

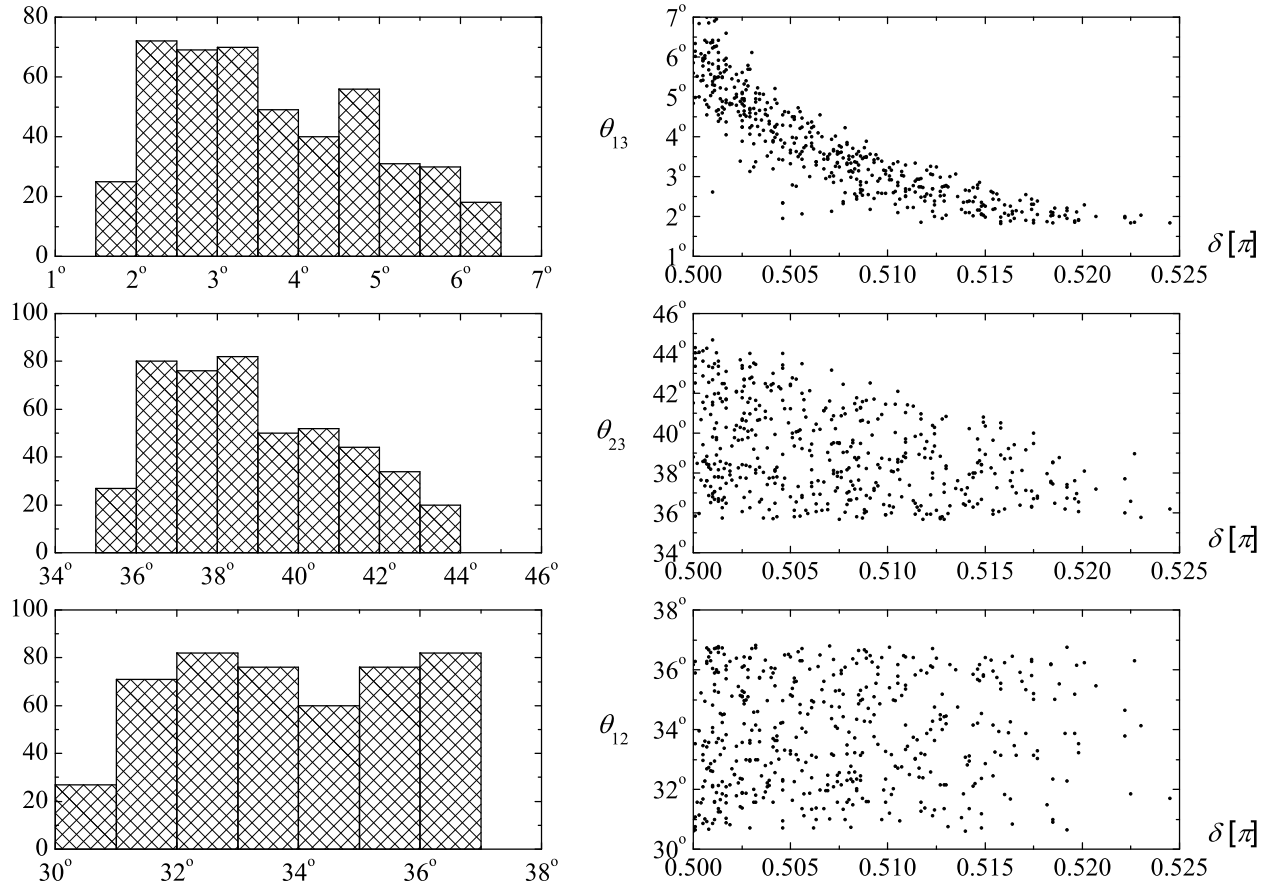


Figure 11: Pattern \mathbf{B}_4 of M_ν : allowed ranges of flavor mixing angles $(\theta_{12}, \theta_{23}, \theta_{13})$ versus the Dirac CP-violating phase δ at the 3σ level, where the probability distribution of three angles are shown in the left panel.

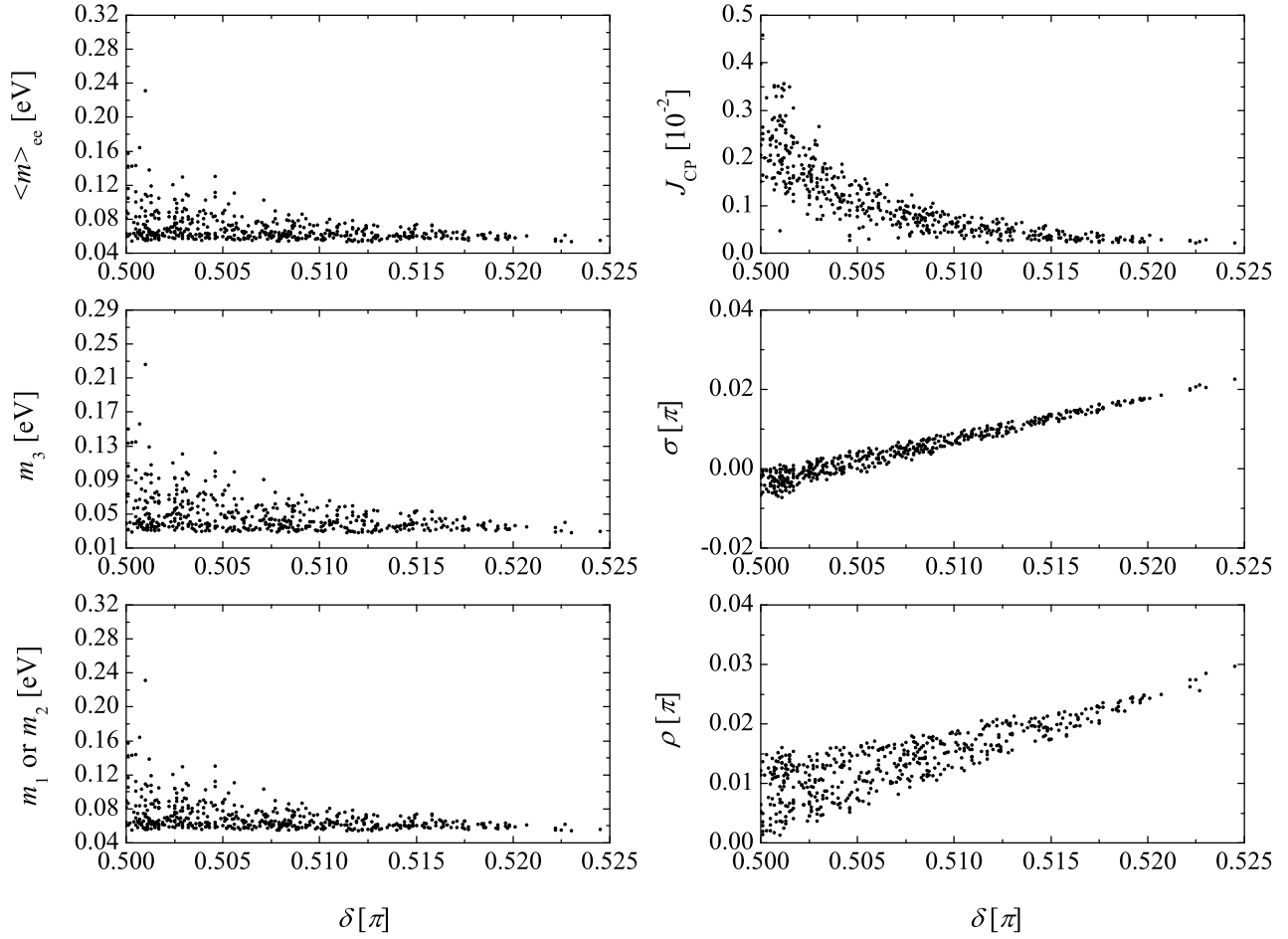


Figure 12: Pattern \mathbf{B}_4 of M_ν : allowed ranges of the neutrino masses (m_1, m_2, m_3), the Jarlskog invariant J_{CP} and the Majorana CP-violating phases (ρ, σ) versus the Dirac CP-violating phase δ at the 3σ level.

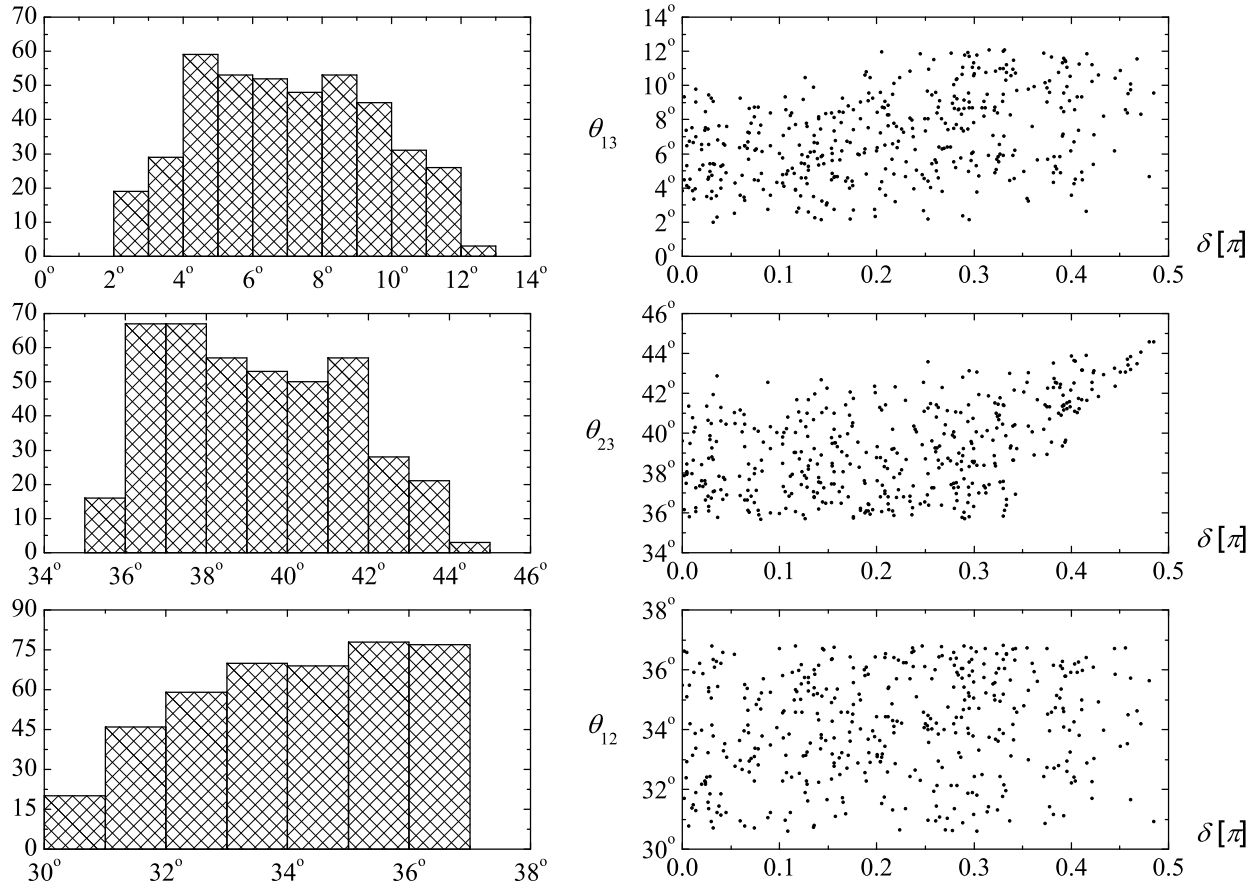


Figure 13: Pattern **C** of M_ν : allowed ranges of flavor mixing angles $(\theta_{12}, \theta_{23}, \theta_{13})$ versus the Dirac CP-violating phase δ at the 3σ level, where the probability distribution of three angles are shown in the left panel.

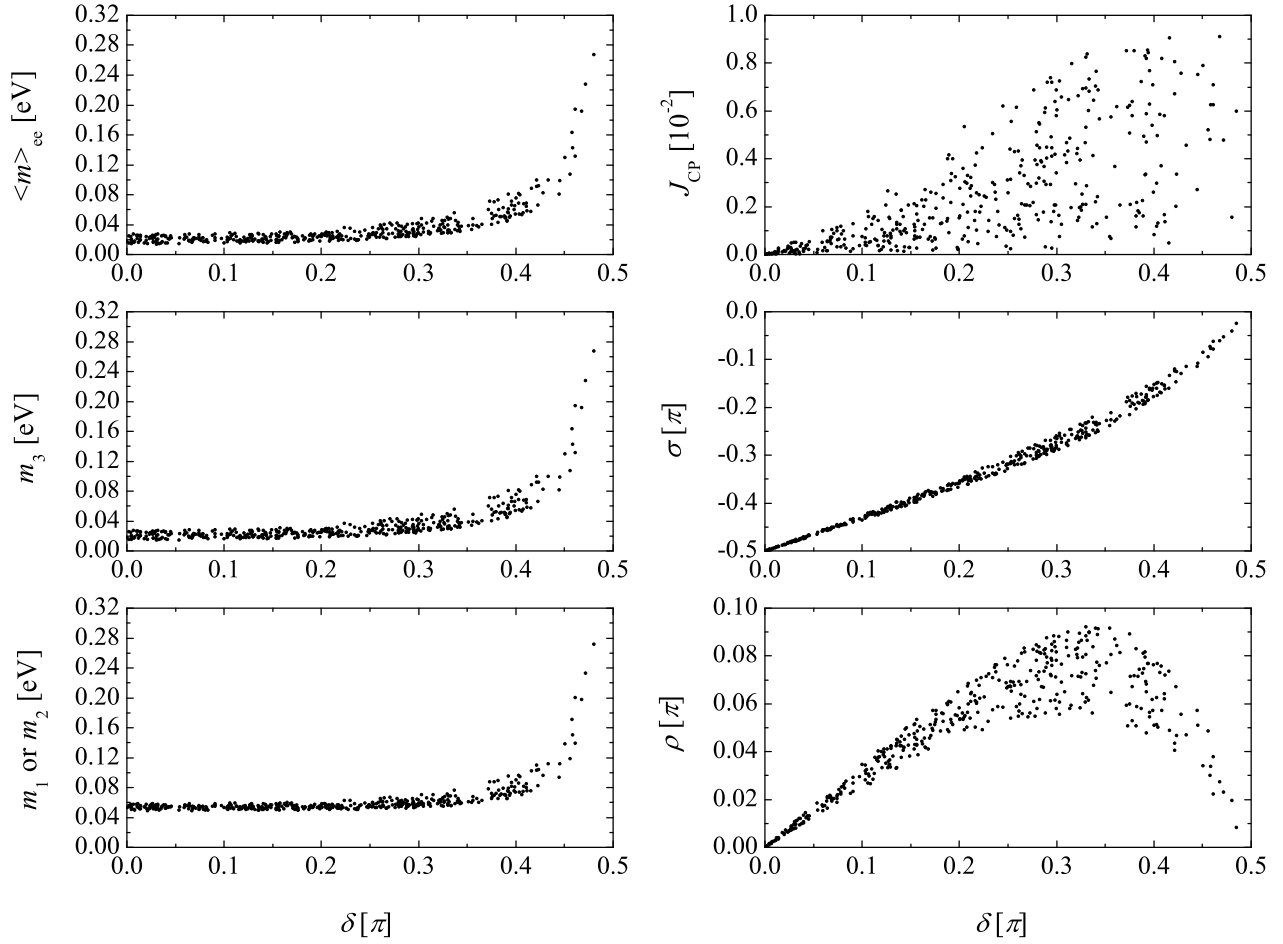


Figure 14: Pattern **C** of M_ν : allowed ranges of the neutrino masses (m_1, m_2, m_3), the Jarlskog invariant J_{CP} and the Majorana CP-violating phases (ρ, σ) versus the Dirac CP-violating phase δ at the 3σ level.